Telomerase-dependent Cell Cycle Regulation Requires NOL1

and

TINF2 mRNA Degradation by HuR Modulates Telomere Function

Juyeong Hong

The Graduate School

Yonsei University

Department of Integrated Omics for Biomedical Science

Telomerase-dependent Cell Cycle Regulation Requires NOL1

and

TINF2 mRNA Degradation by HuR Modulates Telomere Function

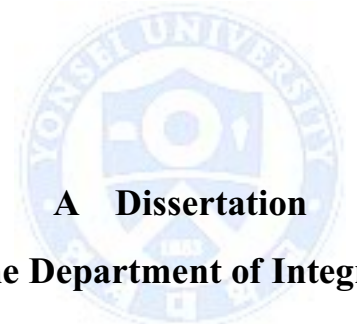

A Dissertation

Submitted to the Department of Integrated Omics for Biomedical Science

And the Graduate School of Yonsei University

In partial fulfillment of the

Requirements for the degree of

Doctor of Philosophy

Juyeong Hong

February 2016

This certifies that the dissertation

Of Juyeong Hong is approved.

_____

Thesis Supervisor: In Kwon Chung

_____

Tae Ho Lee

_____

Jin Won Cho

_____

Jong Bok Yoon

_____

Hyun Soo Cho

The Graduate School

Yonsei University

January 2016

Acknowledgements

우선 지난 5년 학위 과정동안 많은 가르침을 주신 저희 지도교수님인 정인권 교수님께 진심으로 감사의 말을 전하고 싶습니다. 학위를 준비하며, 많은 실패와 역경이 있었지만, 교수님의 지도와 격려, 그리고 실험실 연구원들의 도움으로 무사히 학위를 마칠 수 있게 되었습니다. 감사드립니다. 그리고 학위논문을 준비함에 있어서 심사와 가르침을 주신 이태호 교수님, 조진원 교수님, 윤종복 교수님, 조현수 교수님께도 감사의 말을 전합니다.

주위에서 격려해주시고 지켜봐 주시는 만큼 더욱 분들께 부끄럽지 않도록, 앞으로 더욱 정진하는 진정한 연구자가 되도록 노력하겠습니다.

감사합니다.

January 2016

Juyeong Hong

Table of Contents

List of Figures

Chapter 1. Telomerase-dependent cell cycle regulation requires NOL1

Chapter 2. TINF2 mRNA degradation by HuR modulates telomere function.

Chapter 1

Telomerase-dependent Cell Cycle Regulation Requires NOL1

1. Abstract

Telomerase is a ribonucleoprotein enzyme that plays a critical role in the maintenance of telomere repeats in most eukaryotic organisms. Although overexpression of telomerase in normal human somatic cells is sufficient to overcome replicative senescence and extend a lifespan, the ability of telomerase to promote tumorigenesis could require additional activities that are independent of its role in telomere extension. Here we identify NOL1 (proliferation-associated nuclear antigen 120) as a TERC-binding protein, which is found in association with catalytically active telomerase. We show that NOL1 binds to cyclin D1 promoter at the TCF binding element and activates its transcription. Moreover, telomerase further enhances expression of cyclin D1 gene by interacting with NOL1 and recruitment to the cyclin D1 promoter, demonstrating a role of telomerase as a modulator of NOL1-dependent transcription in human cancer cells. These data suggest that NOL1 could represent a novel mechanism by which telomerase promotes the prolonged expression of growth-promoting genes critical for the maintenance of tumor survival and cell proliferation. (Chi and Delgado-Olguin 2013)

These data suggest that a functional interplay between NOL1 and telomerase plays a critical role in bypassing checkpoint signaling pathways and maintaining cell proliferation capacity, essential properties of telomerase required for cancer progression.

2. Introduction

Telomeres, the highly specialized nucleoprotein complexes located at the ends of eukaryotic chromosomes, are essential for maintenance of chromosome stability and genome integrity (Blackburn, 2001; Smogorzewska and de Lange, 2004). Telomeric DNA is tightly associated with the six-subunit protein complex shelterin which is composed of TRF1,TRF2, TIN2, TPP1, POT1, RAP1 and prevents chromosomal ends from being recognized as DNA damage (Liu et al., 2004; de Lange 2005; Palm and de Lange 2008; Sfeir and de Lange 2012). TRF1 and TRF2 directly bind to telomeric DNA containing myb DNA-binding domain and an internal TRFH homodimerization domain (de Lange 2009). Loss of TRF2 leads to cell cycle arrest and activation of ATM kinase at telomeres. TINF2 links TRF1 and TRF2, and it also binds to TPP1 that interacts with 3' single-stranded overhang binding protein POT1. Depletion of POT1 induces phosphorylation of ATR target Chk1 (de Lange 2007). In the absence of a telomere maintenance pathway, most human somatic cells show a progressive loss of telomeric DNA with each round of cell division due to the end replication problem (Lingner et al., 1995; Blasco et al., 1997). The maintenance of telomere repeats in most eukaryotic organisms requires telomerase, which adds telomere repeats onto the 3' ends of linear chromosomes by reverse transcription (Autexier and Lue 2006; Bianchi and Shore 2008). Human telomerase consists of telomerase reverse transcriptase (hTERT), telomerase RNA component (TERC), and several additional proteins including dyskerin, TCAB1, pontin, and reptin (Egan and Collins 2012; Venteicher et al., 2009; Venteicher et al., 2008). Telomerase expression is very low in most human somatic cells but upregulated in many human cancer cells and stem cells. Thus, telomerase plays critical roles in continued cell proliferation and

tumorigenesis by maintaining telomere integrity and homeostasis (Kim et al., 1994; Bodnar et al., 1998; Hahn et al., 1999).

Although overexpression of telomerase is sufficient to overcome replicative senescence (Bodnar et al., 1998), recent studies have revealed that besides its reverse transcriptase activity, telomerase has the noncanonical functions, which contribute to cancer development and progression (Stewart et al., 2002; Li and Tergaonkar, 2014). Ectopic expression of telomerase in human mammary epithelial cells resulted in enhanced expression of growth-promoting genes (Smith et al., 2003). Transgenic induction of TERT in mouse skin epithelium was shown to cause proliferation of quiescent stem cells (Sarin et al., 2005). Intriguingly, this function for TERT is independent of reverse transcriptase activity and of TERC (Choi et al., 2008). Furthermore, it has been reported that TERT directly interacts with BRG1 and activates Wnt/β-catenin-dependent genes such as cyclin D1 and c-Myc (Park et al., 2009). Although these data provide evidence to the nontelomeric functions of telomerase, the proposed noncanonical role of TERT in Wnt/β-catenin signaling cascade has been controversial. Several recent studies have reported a lack of physical association of hTERT with BRG1 or β-catenin (Listerman et al., 2014) as well as no apparent effect of TERT deficiency on phenotypes associated with Wnt signaling in TERT knockout mice (Strong et al., 2011). These findings suggest that hTERT may enhance the expression of growth-promoting genes, but this event may not be solely promoted by Wnt signaling. Indeed, hTERT has been reported to bind to NF-κB p65 subunit and regulate NF-κB-dependent gene expression by recruitment to specific target promoters (Ghosh et al., 2012). In addition, TERT forms a complex with RMRP to act as an RNA-dependent RNA polymerase (RDRP) (Maida, Y. et al., 2009). TERT-RMRP-RDRP complex produces RMRP-derived double-stranded RNAs (dsRNAs) that are further processed

into small interfering RNAs (siRNAs), which in turn regulate gene expression. As telomerase has regulatory roles in the expression of genes in cancer development and progression, a better understanding of biochemical properties of telomerase could provide improved therapeautic strategies in cancer treatment.

Since the large size of active human telomerase suggests the existence of additional components, we performed a large scale affinity purification to identify proteins that interact with telomerase. Here we identify NOL1 (proliferation-associated nucleolar antigen p120) as a TERC-binding protein. NOL1 was identified as a RNA-binding and nucleolar-specific protein, which is highly expressed in the majority of human malignant tumor cells but not detectable in normal resting cells (Ochs et al., 1988; Jhiang et al., 1990; Fonagy et al., 1992; Fonagy et al., 1993). NOL1 is expressed early in the G1 phase and reaches its peak during early S phase, suggesting it may be involved in the regulation of cell cycle. Although NOL1 has been implicated as a tumor cell marker (Gorczyca et al., 1992), the molecular mechanism by which NOL1 contributes to tumorigenesis is poorly understood. In this work, we investigated a role of NOL1 and demonstrated that it binds to cyclin D1 promoter at the TCF binding element and activates its transcription. Furthermore, we show that telomerase associates with NOL1 via TERC and localizes to the cyclin D1 promoter in a NOL1-dependent manner, demonstrating a regulatory role of telomerase as a transcriptional modulator in human cancer cells. These data provides further insight to the noncanonical functions of telomerase and suggest potential intervention for telomerase-targeted cancer therapy.

3. Materials and methods

Cell culture

Human cervical carcinoma HeLa S3 cells and human embryonic kidney 293cells were grown in Dulbecco's modified Eagle's medium containing 10% fetal bovine serum with 100 units/mL penicillin, and 100 μg/mL streptomycin in 5% CO2 at 37 °C. Human osteosarcoma U2-OS cells were grown in McCoy's modified medium with10% fetal bovine serum, 100 units/mL penicillin, and 100 μg/mL streptomycin in 5% CO2 at 37 °C.

Constructs

The Nol1 expression vectors were constructed into pcDNA 3.1 V5/His or pCMV 3X flag. The human Cyclin D1 promoter luciferase plasmids (originally obtained from Richard Pestell) were subcloned into pGL4.20 puro -luc (promega).

Direct telomerase activity assays.

Telomerase was immunopurified from cell extracts using the indicated antibodies. The reaction mixture (50 μl) contained TRAP reaction buffer (300 mM Tris-HCl, pH 8.3, 960 mM KCl, 23 mM MgCl2, 7.5 mM EDTA, pH 8.0, 0.05% Tween-20), 0.1 μM HTS primer, 0.1 mM dNTP with immunopurified telomerase complex on beads. Reactions were performed at 37°C for 20min and stopped by heat inactivation at 75°C. TRAP reaction samples were amplified by PCR. PCR was performed using the HTS primer and HACX primer for 30 cycles (denaturation at 94°C for 30 s, annealing at 62°C for 30 s, and extension at 72°C for 30 s). As an internal telomerase assay standard, NT and TSNT primers were added to the PCR mixture

as described previously. The amplified samples were loaded onto a 12% polyacrylamide non-denaturing gel for electrophoresis. After electrophoresis, the gel was stained with SYBR Green (Molecular Probes). The signal intensity was quantified with a LAS-4000 PLUS Image analyzer (Fuji Photo Film).

Transient transfection, immunoprecipitation and immunoblot.

HEK293 cells were transfected with following constructs using Lipofectamine 2000 according to the manufacturer's instruction(invitrogen). 24 hours after transfection, the cells were harvested.

For immunoblotting, whole-cell lysates were prepared using lysis buffer (0.5% NP-40, 0.5% Triton-X100, 150mM NaCl, 2mM EDTA(pH 8.0), 50mM Tris-HCl (pH7.5), 10% glycerol, and Proteinase inhibitor cocktail (Roche)) for 15 min at 4°C, followed by centrifugation (16,000 x g, 10 min). Supernatant fractions were denatured with 5X SDS sample buffer at 98°C for 7 min, seperated by SDS–PAGE and transferred onto PVDF membrane. For immunoblot blocking, 5% skim milk in TBS-T (25mM Tris-HCl, pH 8.0, 125mM NaCl, 0.5% Tween-20) was used and primary antibodies were incubated overnight at 4°C. And then, membranes were washed 3 times in TBS-T, incubated for 1 hr in secondary antibody(Genedepot), washed 3 times and developed with ECL (Santa Cruz) solution. For immunoprecipitation, the cells were lysed with lysis buffer for 15 min at 4°C, followed by spinning at 16,000 x g for 10 min. The cell lysates were pre-cleared with protein A sepharose (GE Healthcare) for 30min. After spinning down, the supernatant was transferred into fresh tubes and incubated with antibodies at 4°C overnight. Subsequently, 40 µl of protein A sepharose was added and incubated for 1 h. Immunoprecipitates were washed 3times with

lysis buffer, then eluted by boiling in loading buffer and analysed by immunoblotting. Primary antibodies were used : anti-Flag(M2, sigma), v5(invitrogen), Nol1(Novus Biologicals), cyclinD1 (abcam), cyclin B1(SantaCruz), c-MYC(SantaCruz), TCAB1 (abcam), dyskerin (SantaCruz), TERT (Rockland), α-tubulin (SantaCruz), TRF1 (Santa Cruz), TRF2 (Cell signaling), RAP1 (Bethyl laboratory), POT1 (abcam), TPP1 (abcam), TIN2 (abcam), p53 (SantaCruz), p21 (SantaCruz), Bcl-2 (SantaCruz), Bax (SantaCruz), Cleaved caspase-3 (Cell signaling).

Dual Luciferase assay

24 hrs after transfection, the cells were harvested. Firefly and Renilla luciferase activities were measured with Victor X5 multi plate reader using a dual luciferase kit (Promega, Madison, WI). The firefly luciferase data for each sample were normalized based on transfection efficiency as measured by Renilla luciferase activity. Each experiment was performed in triplicate and repeated at least three times.

Stable cell line generation using retroviral expressing vector.

Phoenix cultures were grown in DMEM/10% bovine growth serum/100 units/mL penicillin, and 100 μg/mL streptomycin. Retroviruses were generated from Pheonix cells by transfecting the retroviral shRNA plasmids by Lipofectamine 2000 (invitrogen). To generate stable cell lines, HeLa S3 cells were transduced with shRNA constructs in the pSUPER.retro.puro vector (Oligogene), selected with 1μg/ml puromycin (GIBCO) for 2 weeks. For shRNA vectors, hairpin sequences were:

sh-NOL1 A 5’-

gatccccGCGTTGCTGCCCATTGAAATTttcaagagaAATTTCAATGGGCAGCAACGCttttta -3’;

sh-NOL1 B 5’-gatccccGGACGATGCTGATACGGTATTttcaagagaAATACCGTATCAGCATCGTCCttttta -3’;

sh-TERT A 5’-gatccccGGGAATTTGGAGTGACCAATTttcaagagaAATTGGTCACTCCAAATTCCCttttta -3’;

sh-TERT B 5’-gatccccCGGTGTACGCCGAGACCAATTttcaagagaAATTGGTCTCGGCGTACACCGttttta -3’.

Semi-quantitative RT-PCR

Total RNA was isolated from HeLa S3 cells using Easy-BLUE (Intron, Korea). cDNA was reverse-transcribed from 1 μg of total RNA using M-MLV Reverse-Transcriptase (Promega) and used for semi-quantitative RT-PCR.

The following primers were used:

TERT F: 5'-CGG AAG AGT GTC TGG AGC AA-3’

TERT R: 5’-GGA TGA AGC GGA GTC TGG A-3’

TERC F: 5'-TCT AAC CCT AAC TGA GAA GGG CGT AG-3’

TERC R: 5'-GTT TGC TCT AGA ATG AAC GGT GGA AG-3’

dykerin F: 5'-ACA GGG TGA AGA GTT CTG GCA CAT-3’

dykerin R: 5'-TGA AGG TGA GGC TTC CCA ACT CAA-3’

Cyclin D1 F: 5´-CAC ACG GAC TAC AGG GGA GT-3’

Cyclin D1 R: 5´-CAC AGG AGC TGG TGT TCC AT-3´

c-Myc F: 5’-AAT GAA AAG GCC CCC AAG GTA GTT ATC C-3’

c-Myc R: 5’-GTC GTT TCC GCA ACA AGT CCT CTT C-3’

GAPDH F: 5'-CTC AGA CAC CAT GGG GAA GGT GA-3’

GAPDH R: 5'-ATG ATC TTG AGG CTG TTG TCA TA -3’

Immunofluorescence and Fluorescence in situ hybridization (FISH)

Cells grown on cover slips were fixed with 4% paraformadehyde in PBS for 10 min and permeabilized in PBS containing 0.5% Triton X-100 for 10 min. Afterwards, cells were blocked in PBG (PBS containing 0.5% BSA,and 0.2% cold fish gelatin) for 10 min. Cells were incubated for 16 hr in PBG at 4°C with the following antibodies: anti-Coilin (abcam), anti-TERT (500ng/mL, Rockland)), anti-nucleolin(SantaCruz). Coverslips were washed 3 times with PBG for 5 min each followed by incubation with Alexa Fluor 488 goat anti-rabbit immunoglobulin, Alexa Fluor 350 goat anti-mouse and Alexa Fluor 568 goat anti-mouse immunoglobulin (Molecular Probes) for 1 hr in PBG at room temperature. Finally, cover slips were washed 3 times with PBG for 5 min each and mounted using VectaShield (DAPI containing, Vector Labs) medium.

For PNA-FISH, Cells grown on cover slips were fixed with 4% paraformadehyde in PBS for 10 min and permeabilized in PBS containing 0.5% Triton X-100 for 10 min. Afterwards, cells were blocked in PBG (PBS containing 0.5% BSA,and 0.2% cold fish gelatin) for 10 min. Cells were incubated for 16 hr in PBG at 4°C with primary anti-bodies. After PBS washes, coverslips were incubated with alexa 488 secondary antibody raised against mouse or rabbit

for 45 min and washed in PBS. At this point, coverslips were fixed with 4% paraformaldehyde for 10 min at RT; washed extensively in PBS; dehydrated consecutively in 70%, 90% , and 100% ethanol for 5 min each; and allowed to dry completely. Hybridization solution (70% formamide, 1mg/ml blocking reagent [Roche], 10Mm Tris-HCl, pH 7.2), containing the peptide nucleic acid(PNA) probe fluorescein isothiocyanate (FITC)-OO-(CCCTAA)3(Applied Biosystems), was added to each coverslip, and the cells were denatured by heating for 10 min at 82°C on a heat block. After 12-14 hr incubation at RT in the dark, cells were washed twice with washing solution (70% formamide, 10mm Tris-HCl, pH7.2) and twice in PBS. DNA was counterstained with DAPI (4',6-diamidino-2-phenylindole) and the images were analyzed by Confocal analyses.

Double thymidine block of HeLa S3 cells

HeLa S3 cells were grown in Dulbecco's modified Eagle's medium (Hyclone) containing 10% fetal bovine serum (Hyclone). Cells in the logarithmic growth phase were incubated in medium containing 2 mM thymidine (Sigma). After 19 h, cells were washed twice with PBS and grown in regular medium for 9 h before a second incubation with 2 mM thymidine for 17 h. Cells released from the second thymidine block were collected at the indicated time.

Chromatin Immunoprecipitation assays

For in vivo ChIP assays, Hela S3 cells were washed twice in cold PBS and immediately cross-linked with 1% formaldehyde for 30 min at room temperature. Formaldehyde was quenched by adding glycine (final 0.125 M concentration). Then cells were homogenized, and processed in ChIP-lysis buffer (50 mM Tris-HCl (pH 8.0), 1% SDS, 10mM EDTA) containing proteinase

inhibitors and further incubated on ice for 15 min. Cell lysates were sonicated to obtain chromatin fragments with an average size of 600 bp, and centrifugated (13,000 rpm, 20 min). Supernatants were removed, diluted with ChIP-dilution buffer (0.01% SDS, 1.1% TritonX-100, 1.2mM EDTA, 16.7mM Tris-HCl(pH8.0), 150mL NaCl, proteinase inhibitor cocktails) and precleared with protein A sepharose bead (GE Healthcare) for 2 hr at 4 °C. Supernatant from precleared lysates was immunoprecipitated with Flag M2 agarose bead (sigma) overnight at 4 °C and pulled down by centrifugation (9,000 rpm, 1min). Immunoprecipitates were further washed serially with low salt wash buffer(0.1% SDS, 1% TritonX-100, 2 mM EDTA, 20 mM Tris-HCl (pH8.1), 150 mM NaCl), high salt (0.1% SDS, 1% TritonX-100, 2 mM EDTA, 20 mM Tris-HCl (pH8.1), 500 mM NaCl), LiCl wash buffer (10 mM Tris-HCl (pH 8.0), 1 mM EDTA, 250 mM LiCl, 1% NP40, 1% deoxycholate) and TE buffer, and eluted with freshly prepared elution buffer (1% SDS, 0.1 M NaHCO3). Finally, immunoprecipitates cross-linked were reversed by incubation at 65 °C overnight and treated with RNase A and proteinase K to extract DNA. The isolated DNAs were analysed by semiquantitative PCR.

The primers used were the following:

Cyclin D1-TBE-F: 5’- CGCTC CCATT CTCTG CCGGG-3’

Cyclin D1-TBE-R: 5’- CCGCG CTCCC TCGCG CTCTT-3’

Cyclin D1-3’UTR-F: 5’- CAAGA GAAGA TTACC GCCCG AG-3’

Cyclin D1-3’UTR-R: 5’- TCCCC AGCCT TTTTG ACACC-3’

c-Myc-TBE1-F: 5’- CGTCT AGCAC CTTTG ATTTC TCCC-3’

c-Myc-TBE1-R: 5’-CTCTG CCAGT CTGTA CCCCA CCGT-3’

c-Myc-3’UTR-F: 5’-CTAAT GTATC ACAAA GTCCT TTA-3’

c-Myc-3’UTR-R: 5’-GTGAT CTGCT CTGTT AGCTT TTGA-3’

Peptide identification using LC-MS/MS

Nano LC–MS/MS analysis was performed with a nano HPLC system (Agilent,Wilmington, DE). The nano chip column (Agilent,Wilmington, DE, 150 mm × 0.075 mm) was used for peptide separation. The mobile phase A for LC separation was 0.1% formic acid in deionized water and the mobile phase B was 0.1% formic acid in acetonitrile. The chromatography gradient was designed for a linear increase from 5% B to 30 B in 25 min, 40% B to 60% B in 5 min, 90% B in 10 min, and 5% B in 15 min. The flow rate was maintained at 300 nL/min. Product ion spectra were collected in the information-dependent acquisition (IDA) mode and were analyzed by Agilent 6530 Accurate-Mass Q-TOF using continuous cycles of one full scan TOF MS from 200-1500 m/z (1.0 s) plus three product ion scans from 50-1800 m/z (1.5 s each). Precursor m/z values were selected starting with the most intense ion, using a selection quadrupole resolution of 3 Da. The rolling collision energy feature was used, which determines collision energy based on the precursor value and charge state. The dynamic exclusion time for precursor ion m/z values was 60 s.

Fluorescence-activated Cell sorter(FACS) Analysis

Hele S3 cells were washed with ice-cold PBS and fixed overnight at 4 °C in ice-cold serially diluted 70% ethanol. The fixed cells were resuspended in PBS containing RNase A (200μg/ml) and propidium iodide(50μg/ml) and incubated in the dark for 30 min at 37 °C. Cell cycle progression was monitored by flow cytometry using a FACScan flow cytometer (BD Biosciences).

4. Results

4.1 Identification of Nol1 as a TERT-interacting factor

hTERT has been known to be involved in cellular proliferation and cancer development through interacting with other proteins. We hoped to find proteins that interact with hTERT, and expressed Flag-tagged hTERT protein in HEK293 cells and isolated hTERT complexes by using large scale affinity purification. Proteins co-purified with Flag-hTERT were identified by nano-liquid chromatography-tandem mass spectrometry (nano LC-MS/MS). Among the known telomerase components, TCAB1 and nucleolin were enriched in the hTERT complexes (Figure 1). In addition, analysis of a band migrating with an approximate relative molecular mass of 120 kDa identified NOL1, a highly conserved, nucleolar-specific, RNA-binding protein (Ochs et al., 1988; Jhiang et al., 1990). Since the NOL1 protein was detected in proliferating tissues but not in normal resting cells, NOL1 has been implicated as a tumor cell marker. Thus, we wanted to investigate the role of NOL1 in telomerase function.

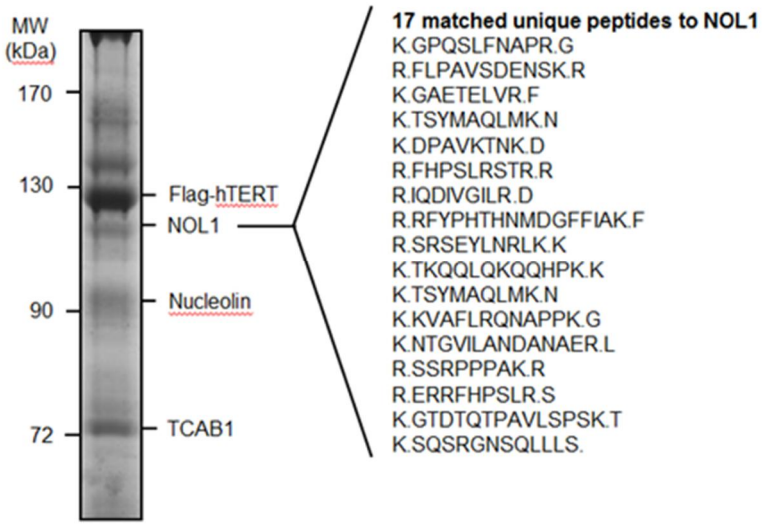

Figure 1. Identification of NOL1 as a TERC-interacting protein. Lysates from HEK293 cells expressing Flag-hTERT were immunoprecipitated with anti-Flag antibody and assayed for protein binding by Coomassie staining of SDS-PAGE gel. Binding proteins were identified by nano LC-MS/MS. Molecular size markers are shown in kilodaltons. Seventeen unique peptides for NOL1 identified from mass spectrometry are shown.

4.2. NOL1 interacts with TERT in vivo.

Since NOL1 was detected in proliferating tissues but not in normal resting cells, it has been implicated as a tumor cell marker. hTERT is also activated in many cancer cells but not in normal somatic cells. Thus, we wanted to investigate the role of NOL1 in telomerase function. To determine whether hTERT and NOL1 associate *in vivo*, HEK293 cells were co-transfected with Flag-hTERT and NOL1-V5 expression vectors and subjected to immunoprecipitation. Co-immunoprecipitation with anti-flag antibody reveals Nol1 association with TERT, bringing down NOL1-V5 (Fig. 1a). Reciprocal immunoprecipitation showed that Flag-hTERT was detected in anti-V5 immunoprecipitates, indicating that hTERT associates with NOL1 in mammalian cells. Interestingly, the interaction between Flag-hTERT and NOL1-V5 was disrupted by RNase A treatment, which degraded TERC. Endogenous NOL1 was specifically bound to endogenous hTERT, and this association was also disrupted by RNase A treatment (Fig. 1b), suggesting that NOL1 associates with hTERT via TERC binding in vivo. These findings were further verified by immunoprecipitation experiments with U2OS cells, which lack endogenous hTERT and TERC[28]. Flag-hTERT did not interact with NOL1-V5 due to a lack of TERC (Fig. 1c). Taken together, these results suggest that NOL1 associates with hTERT via TERC *in vivo*.

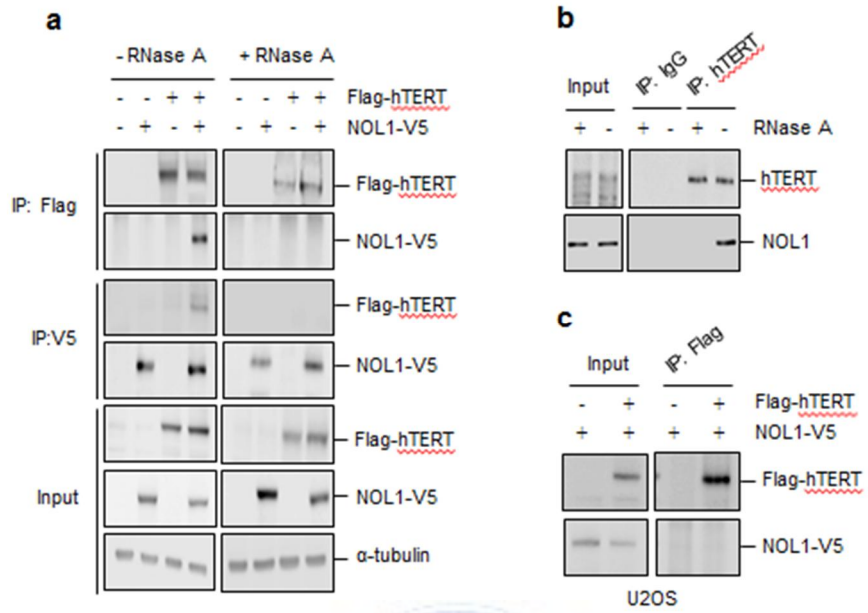

Figure 2. NOL1 interacts with TERT via TERC *in vivo* (a) HeLa S3 cells expressing Flag-hTERT and NOL1-V5 were subjected to immunoprecipitation (IP) with anti-Flag and anti-V5 antibodies, followed by immunoblotting with anti-V5 and anti-Flag antibodies. The extracts were treated with 0.1 mg/ml RNase A during immunoprecipitation to degrade TERC. (b) HeLa S3 cells were subjected to IP with anti-hTERT antibody, followed by immunoblotting with anti-NOL1 antibody. IgG was used as a negative control. (c) Telomerase-negative U2OS cells expressing Flag-hTERT and NOL1-V5 were subjected to IP with anti-Flag antibody, followed by immunoblotting with anti-V5 antibody.

4.3 Domain mapping of TERT and Nol1 for their interaction

hTERT has four functional domains. The N-terminal domain(TEN) is involved in telomerase recruitment to telomeres and telomere synthesis. The TERT RNA binding domain(TRBD) contains several RNA binding sequences required for TERC binding. The reverse transcriptase domain is important for its catalytic activity of the enzyme. The CTE domain plays a role in protein-protein interaction and telomerase localization.

Our data has shown that hTERT associates with NOL1. To better characterize this interaction, we mapped the domain in TERT that mediates the interaction with NOL1. To determine the domain in hTERT that is responsible for NOL1 interaction, we assessed binding of NOL1-V5 by immunoprecipitating a series of deletion fragments of hTERT (Fig. 3a). NOL1-V5 was immunoprecipitated only by the hTERT fragments containing amino acid residues 1-589 (Fig. 3b). Since this region contains the TERC-binding domain, we examined whether this domain is essential for NOL1 binding to hTERT. The results showed that removing the TERC-binding domain on hTERT abolished NOL1 binding (Fig. 3c,d), further supporting that the association of NOL1 with hTERT is mediated by TERC. To investigate the domain of NOL1 that is required for TERC binding, we generated deletion constructs lacking a coiled-coil domain or a putative rRNA methyltransferase domain[29,30] (Fig. 3e). HEK293 cells were co-trasnfected with Flag-hTERT and a deletion construct of NOL1-v5 and subjected to immunoprecipitation. Flag-hTERT immunoprecipitated NOL1 fragments contaning amino acid residues 380-583 (Fig. 3f), indicating that the putative rRNA methyltransferase domain is essential for hTERT binding.

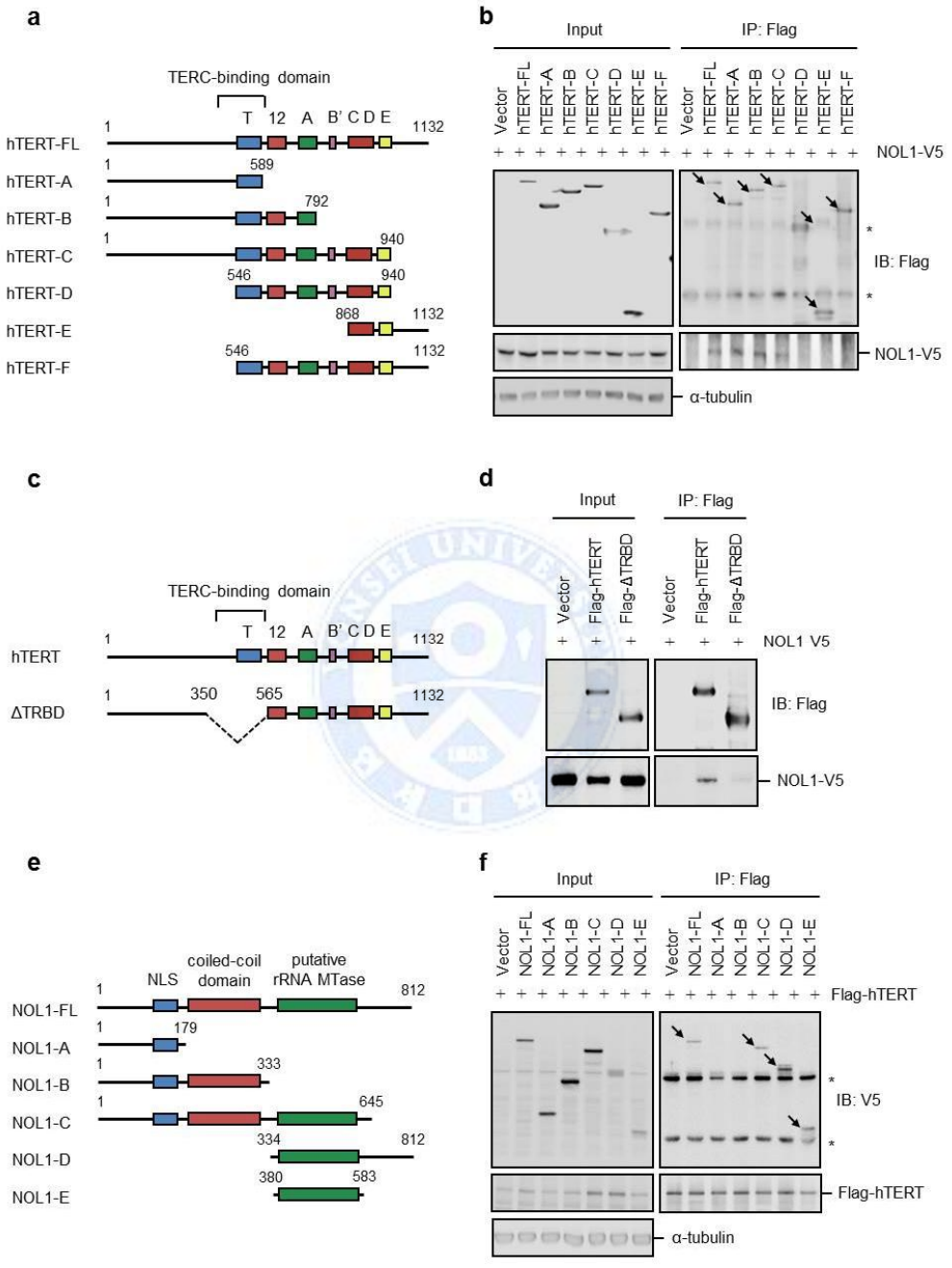

Figure 3. Identification of the domains in NOL1 and hTERT that are required for their

interaction. (a) Schematic representation of the region of hTERT involved in NOL1 binding. TRBD, TERC-binding domain. (b) Lysates from HeLa S3 cells expressing the various Flag-hTERT domains and NOL1-V5 were immunoprecipitated with anti-Flag antibody, followed by immunoblotting with anti-NOL1 antibody. The Flag-TERT domains were indicated by arrows. The asterisks mark the positions of nonspecific immunoglobulin chains. (c) Schematic representation of mutant construct of hTERT in which the TRBD was deleted (ΔTRBD). (d) Removing the TRBD on hTERT abolishes NOL1 association. Lysates from HeLa S3 cells expressing either Flag-hTERT or Flag-ΔTRBD were immunoprecipitated with anti-Flag antibody, followed by immunoblotting with anti-V5 antibody. (e) Schematic representation of the region of NOL1 involved in hTERT binding. The approximate positions of nuclear localization signal (NLS), coiled-coil domain, and putative rRNA methyltransferase (MTase) motif are indicated (f) Lysates from HeLa S3 cells expressing the various NOL1-V5 domains and Flag-TERT were immunoprecipitated with anti-Flag antibody, followed by immunoblotting with anti-V5 antibody. The NOL1-V5 domains immunoprecipitated with Flag-hTERT were indicated by arrows. The asterisks mark the positions of nonspecific immunoglobulin chains.

4.4 NOL1 associates with catalytically active telomerase but does not affect telomerase enzymatic activity.

Since NOL1 associates with hTERT via TERC binding, it is possible that NOL1 may be a telomerase holoenzyme subunit. To address this question, HEK293 cells were co-transfected with NOL1-V5 and either Flag-hTERT or Flag-TCAB1 or Flag-dyskerin and subjected to immunoprecipitation. The results showed that NOL1-V5 was immunoprecipitated by Flag-TCAB1 and Flag-dyskerin, as observed in Flag-hTERT (Figure 4a). We next examined whether NOL1 associates with catalytically active telomerase. HEK293 cells were transfected with Flag-NOL1 or other Flag-tagged telomerase components, subjected to immunoprecipitation with Flag-antibody, and analyzed for telomerase activity by TRAP assay. Immunoprecipitates of Flag-NOL1 contained telomerase activity (Figure 4b), as did those of Flag-hTERT, Flag-TCAB1, and Flag-dyskerin, suggesting that NOL1 is a component of catalytically active telomerase.

To investigate whether NOL1 is involved in canonical telomerase function, the expression of endogenous NOL1 was stably depleted in HeLa S3 cells using short hairpin RNA (shRNA) produced from a retroviral vector. NOL1 depleted cells maintained the reduced levels of NOL1 throughout the duration of the experiments (see below). Knockdown of NOL1 did not affect the levels of telomerase components and shelterin proteins which are responsible for telomere protection and maintenece (Figure 4c and 4d). When NOL1 knockdown cells were analyzed for telomerase activity by TRAP assay, telomerase activity was not influenced by the expression levels of NOL1 (Figure 4e). Taken together, these data indicate that although NOL1 associates with catalytically active telomerase, it has no direct regulatory effect on

telomerase enzymatic activity.

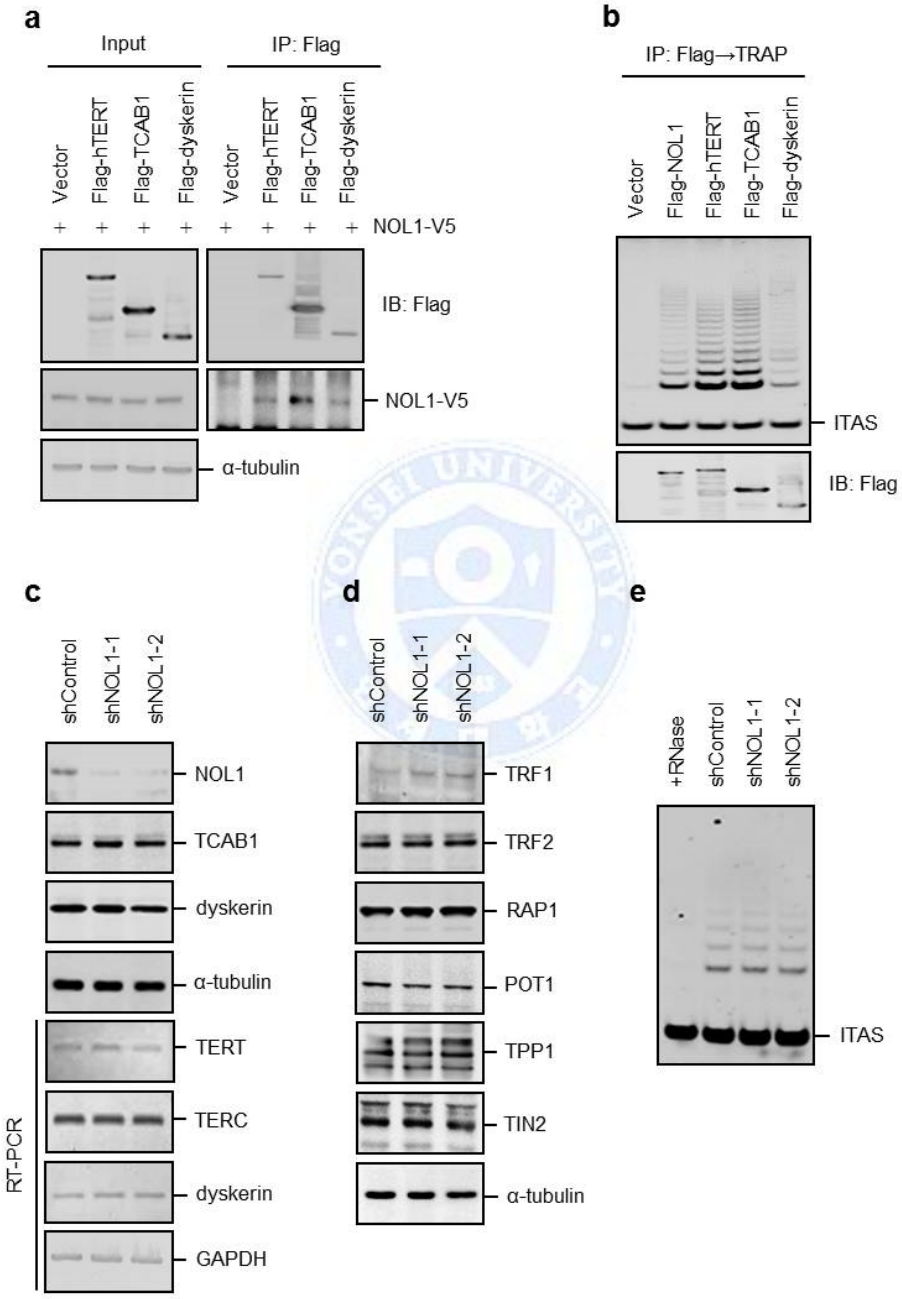

Figure 4. NOL1 associates with catalytically active telomerase. (a) Lysates from HeLa S3 cells expressing NOL1-V5, together with Flag-hTERT, Flag-TCAB1 or Flag-dyskerin were immunoprecipitated with anti-Flag antibody, followed by immunoblotting with anti-V5 antibody. (b) Lysates from HeLa S3 cells expressing Flag-NOL1, Flag-hTERT, Flag-TCAB1 or Flag-dyskerin were immunoprecipitated with anti-Flag antibody and analyzed for telomerase activity by the TRAP assay. ITAS, internal telomerase assay standard. (c) HeLa S3 cells expressing control shRNA (shControl) or NOL1 shRNAs (shNOL1-1 and shNOL1-2) were subjected to immunoblotting to measure the protein levels of telomerase components and quantitative RT-PCR to detect the mRNA levels of telomerase components and TERC. (d) HeLa S3 cells expressing shControl or shNOL1 were subjected to immunoblotting to measure the levels of shelterin proteins. (e) HeLa S3 cells expressing shControl or shNOL1 were analyzed for telomerase activity by the TRAP assay. ITAS, internal telomerase assay standard.

4.5 NOL1 does not influence the subnuclear localization of telomerase.

Telomerase undergoes a highly elaborate, stepwise process of assembly and trafficking within the nucleus (Lee et al., 2014). Human telomerase containing TERC is targeted to cajay body by interacting with TCAB1 and recruited to teloemeres. If NOL1 is required for assembly and trafficking of active telomerase, we would expect that depletion of NOL1 impairs subnuclear localizations of the telomerase components. To test this hypothesis, we depleted NOL1 in HeLa S3 cells and performed indirect immunofluorescence staining to monitor the subnuclear localization of endogenous hTERT. Since telomerase synthesizes telomeres specifically during S phase (Lee et al., 2010; Tomlinson et al., 2006), HeLa S3 cells were synchronized at S phase using double thymidine blockade (Lee et al., 2010). In the control cells, we observed the majority of hTERT was found to localize to nucleoli (Supplemental Figure S1A and S1B). NOL1 depletion does not affect the nucleolar localization of hTERT. Telomerase has been shown to accumulate in Cajal bodies prior to telomere elongation (Venteicher et al., 2009; Venteicher and Artandi 2009). Thus, we investigated whether NOL1 depletion affects co-localization of hTERT with Cajal bodies during S phase. Dual indirect immunofluorescence staining with a coilin-specific antibody and hTERT antibody showed that cajal body localization of hTERT was not influenced by NOL1 depletion.(Supplemental Figure S1C and S1D). These results indicate that NOL1 does not affect the intranuclear trafficking of hTERT.

Dysfunctional telomeres are known to express DNA-damage response factors including γH2AX and 53BP1, and the resulting telomere dysfunction-induced foci (TIFs) represent the foci of DNA-damage response factors that coincide with telomeres (Takai H et al., 2003;

d'Adda di Fagagna et al., 2003; Karlseder et al., 1999). To investigate whether NOL1 depletion may induce telomere-damage pathway, the telomeric foci was examined with using telomeric-DNA containing PNA probe and either anti-γH2AX or anti-53BP1 in NOL1 knockdown and control cell lines. Depletion of NOL1 did not induce telomere-damage foci in the nucleus compared with the control cells (Supplemental Figure S2A and S2B), indicating that NOL1 is not implicated in regulating the DNA-damage response at telomeres.

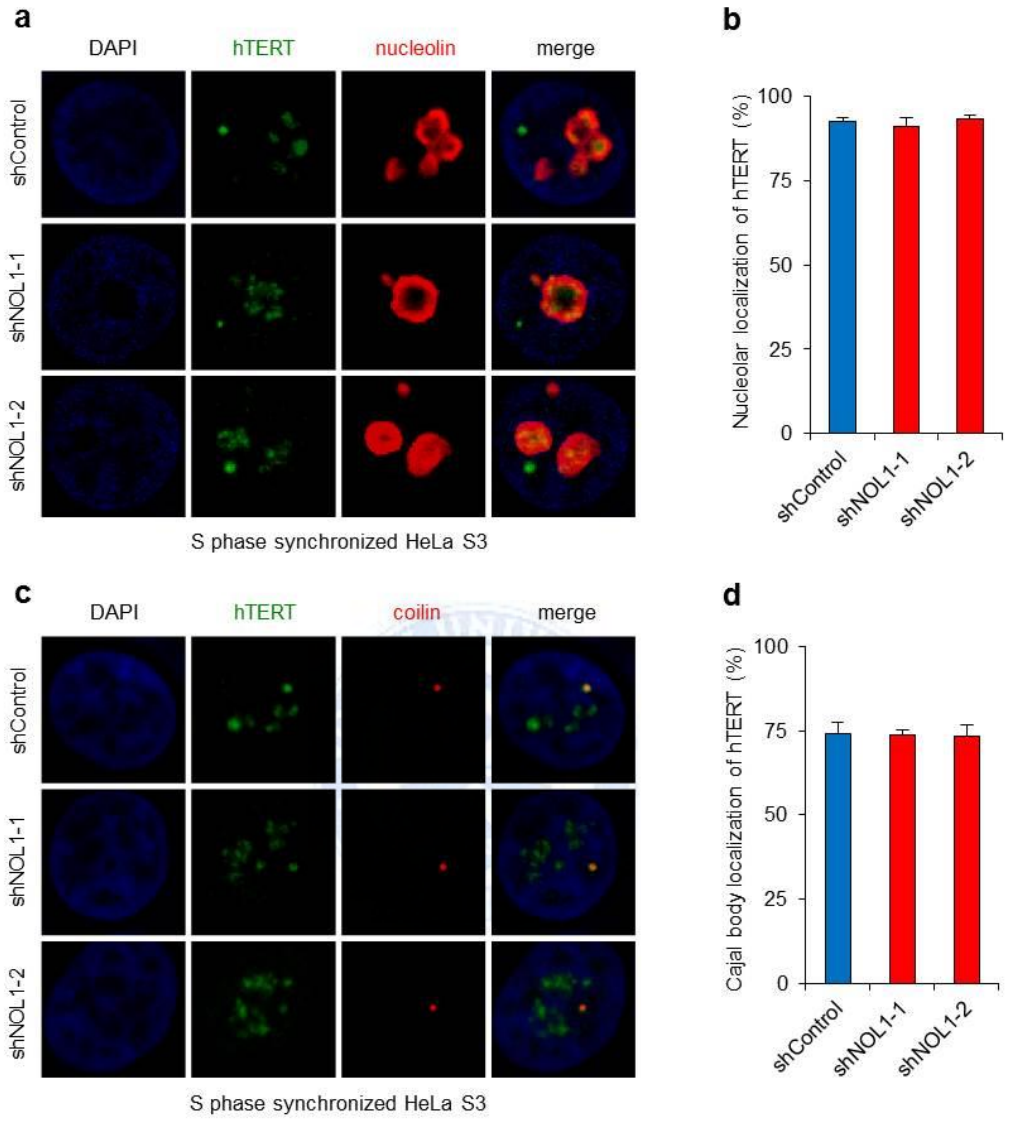

Supplemental Figure 1. Subcellular localization of hTERT is not affected by NOL1 depletion. (a) Colocalization of hTERT(green), nucleolin(red) in S-phase synchronized Hela S3- shControl and shNOL1 cell lines. (b) quantified colocalization of hTERT/nucleolin (mean and s.d. of triplicate experiments; n≥150). (c) colocalization of hTERT and coilin(red). (d) quntifed colocalization of hTERT/coilin. (nucleolin as a specific marker for nucleoli; coilin as

a specific marker for cajal bodies; DNA stained with DAPI (blue); 4',6'-diamidino-2-phenylindole).

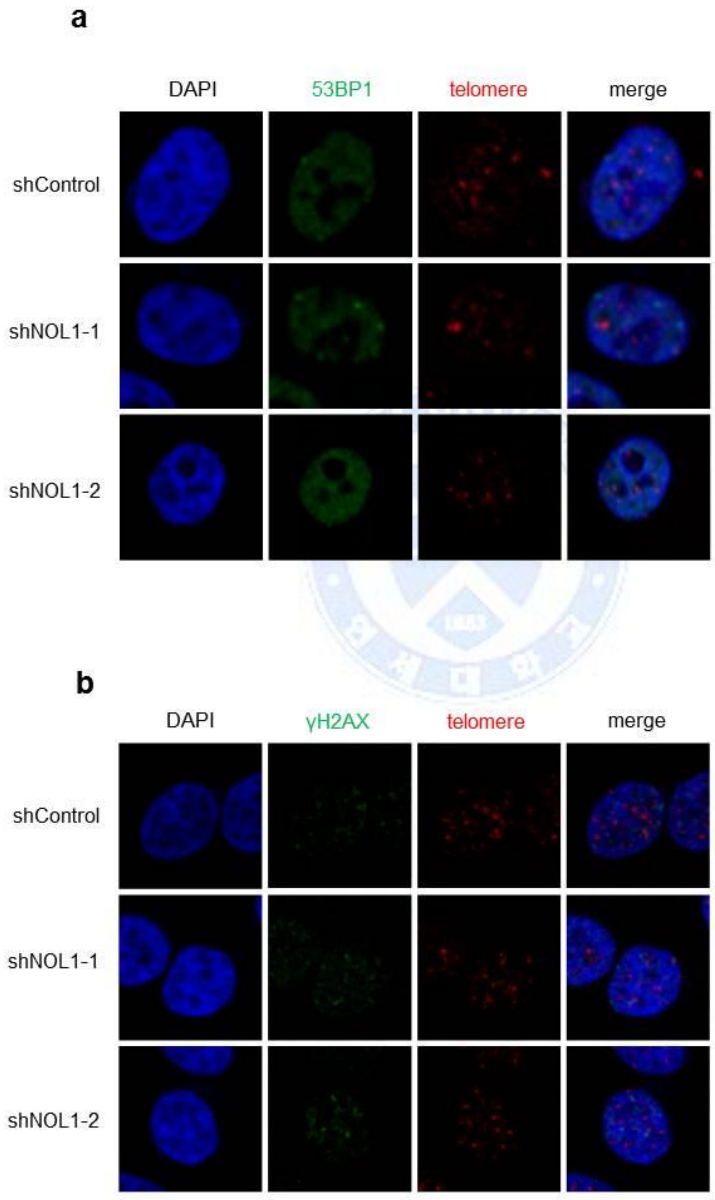

Supplemental Figure 2. NOL1 depletion does not induce TIF formation. (a)

Colocalization of 53BP1(green) and PNA (telomere, red) in HeLa S3 shvector or sh NOL1 cell lines. (b) Colocalization of γH2AX(green) and PNA (telomere, red) in HeLa S3 shvector and shNOL1 cell lines.

4.6 Nol1 activates transcription of cyclin D1.

NOL1 is a proliferation-associated nucleolar protein, which is highly expressed in the majority of human malignant tumors and proliferating cells (Ochs et al., 1988; Jhiang et al., 1990). NOL1 is expressed in the early G1 phase and peaks in S phase, suggesting the possibility that NOL1 might be involved in cell cycle regulation (Fonagy et al., 1992; Fonagy et al., 1993; Gorczyca et al., 1992). Although the expression of NOL1 was shown to be induced rapidly following growth stimulation and produce tumors in the nude mice (Perlaky et al., 1992), the mechanisms by which NOL1 exerts these effects reamin poorly understood. To provide the further insight into the cell cycle and proliferation-related effect of NOL1, we investigated the effect of NOL1 depletion on the expression of cell cycle-dependent and proliferation-controlling genes such as cyclin D1 and c-Myc (Musgrove et al., 2011; Sears, 2004). Depletion of NOL1 resulted in a clear reduction in the expression of cyclin D1 as shown by immunoblot analysis. Similar to this data, we found that the level of cyclin D1 mRNA was also decreased by NOL1 knockdown as demonstrated by RT-PCR experiments, suggesting that NOL1 regulates the expression of cyclin D1 gene at transcriptional level (Figure 5a). In contrast, the expression of c-Myc was not affected by NOL1 depletion, implying that the regulation by NOL1 is promoter specific. Several studies have suggested that hTERT has a non-telomeric function in the gene regulation. Since it has been reported that telomerase modulates Wnt/β-catenin signaling by serving as a transcriptional cofactor in Wnt target genes (Park et al., 2009), we examined whether TERT is implicated in NOL1- mediated transcriptional activation of Cyclin D1 gene. The effect of NOL1 depletion on the cyclin D1 expression was evaluated in U2OS cells, which lack endogenous hTERT and TERC.

Consistent with the data seen in Hela S3 cells (Figure 5a), similar results were obtained in U2OS cells (Figure 5b), suggesting that NOL1-dependent activation of cyclin D1 transcription occurs regardless of telomerase expression.

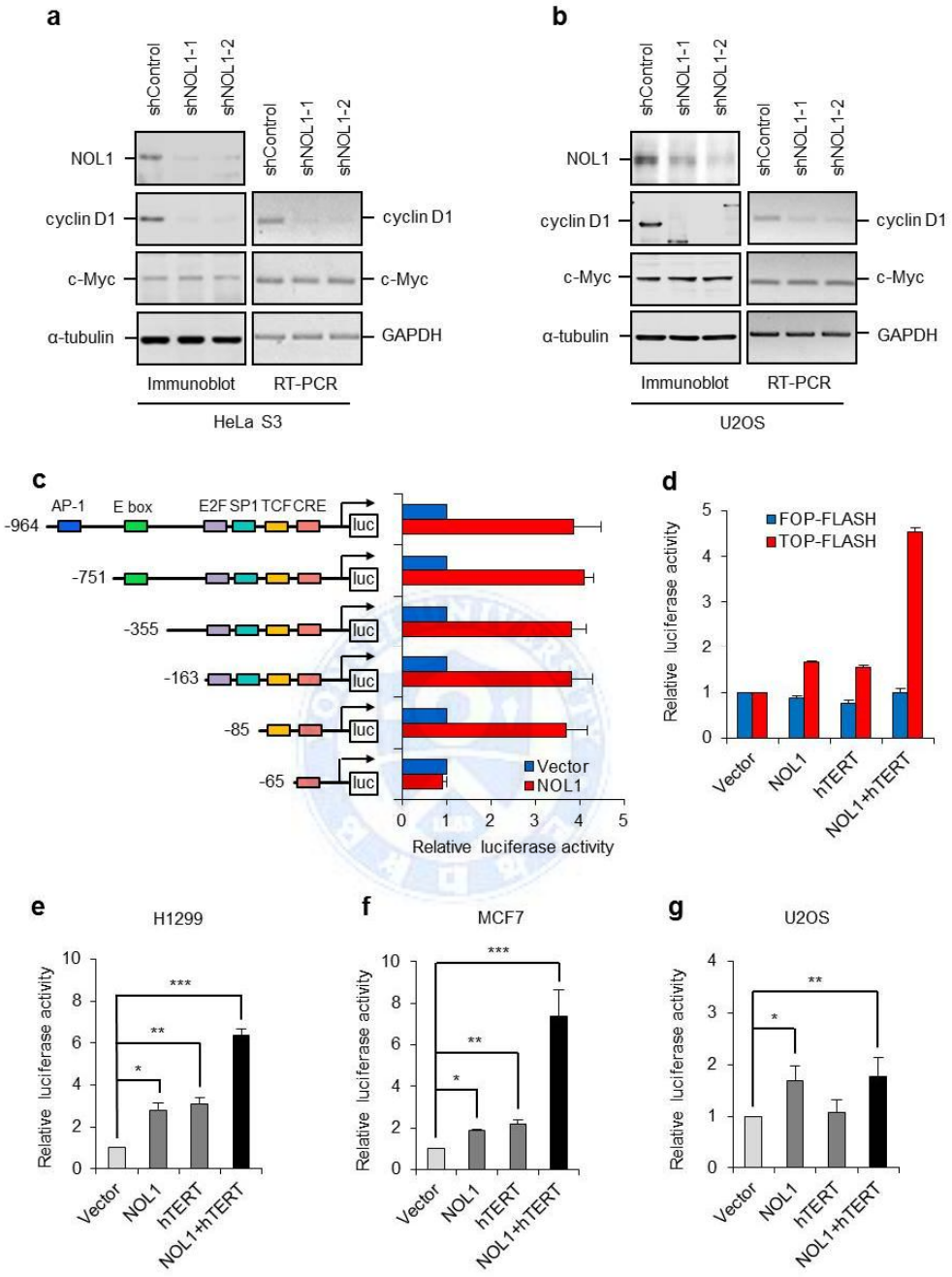

Figure 5. hTERT stimulates transcription of cyclin D1 gene through the interaction with NOL1. (a) HeLa S3 and (b) U2OS cells expressing shControl or shNOL1 were subjected

to immunoblotting to measure the protein levels of cyclin D1 and c-Myc and quantitative RT-PCR to detect the mRNA levels. (c) The structures of the promoter luciferase constructs containing various lengths of upstream fragments in cyclin D1 gene are shown on the left. The binding sites of known transcription factors are indicated. The results of the luciferase assay are shown on the right. HeLa S3 cells were transfected with the promoter luciferase constructs together with Flag-NOL1 or empty vector. The firefly luciferase activity was normalized against the Renilla luciferase activity. Error bars show the standard deviation from the mean of three independent experiments. (d) The effects of TCF transcriptional activity after NOL1 or hTERT overexpression. HeLa S3 cells were transfected with TOP-flesh or FOP-flesh luciferase reporter vectors together with Flag-NOL1, Flag-hTERT or both. The firefly luciferase activity was normalized against the Renilla luciferase activity. Error bars show the standard deviation from the mean of three independent experiments. (e-g) The luciferase assay in H1299 (e), MCF7 (f) and U2OS (g) cells transfected with -964 promoter luciferase reporter vector together with Flag-NOL1, Flag-hTERT or both.

4.7 Telomerase stimulates transcription of cyclin D1 gene through the interaction with NOL1.

The cyclin D1 promoter contains several distinct transcription factor binding sites targeted by different signaling pathways[40]. To determine the NOL1 responsive element, Hela CCL2 cells were transfected with a series of cyclin D1 promoter deletion constructs in the presence of NOL1. Luciferase assay data showed that the cyclin D1 transcription was activated about 4-fold by NOL1 overexpression compared to the vector control (Fig. 5c). The proximal 85-base region, which contains TCF binding site (TBE), is essential for activation of the cyclin D1 promoter, indicating that the NOL1 occupies the TBE region in the cyclin D1 promoter.

We next confirmed the effect of NOL1 overexpression on TCF binding activity by transfecting NOL1 expression with either a TCF-sensitive luciferase reporter vector (TOP-FLASH) or a TCF-insensitive control vector (FOP-FLASH) in HeLa CCL2 cells. The results showed that the ectopic expression of NOL1 upregulated TOP-Flash activity but not FOP-Flash activity (Fig. 5d). Interestingly, ectopic expression of hTERT alone was also able to induce TOP-Flash activity, which was further enhanced by co-expression of NOL1. To verify these findings, telomerase-positive H1299 and MCF7 cells were transfected with the -964 promoter-luciferase reporter vector together with Flag-NOL1 or Flag-hTERT or both. Overexpression of either NOL1 or hTERT led to an increase in cyclin D1 promoter activity compared to the vector control (Fig. 5e,f). When both proteins were co-expressed, we observed an additive effect on cyclin D1 promoter activity. These results suggest that both NOL1 and hTERT are required for the cyclin D1gene transactivation.

Although NOL1 stimulates transcription of cyclin D1 gene independently of hTERT, it is unclear whether hTERT alone is sufficient to activate cyclin D1 promoter activity without

NOL1 association. To test this possibility, we examined dependence of NOL1 in telomerase-negative U2OS cells. As shown in Fig. 5g, cyclin D1 promoter activity was enhanced by NOL1 overexpression but not by hTERT overexpression. Moreover, the additive effect was not observed by co-expression of both proteins. Since hTERT cannot associate with NOL1 in the absence of TERC (Fig. 2c), these findings could result from a lack of TERC in U2OS cells. Taken together, these data suggest that telomerase promotes transcription of cyclin D1 gene through the association with NOL1.

4.8 NOL1 and hTERT associate with the cyclin D1 promoter at the TCF binding site.

As NOL1 and TERT activate the TCF region of the cyclin D1 promoter, we wished to determine whether both NOL1 and hTERT are recruited to the TCF binding site of cyclin D1 promoter. Thus, we carried out chromatin immunoprecipitation (ChIP) to investigate TBE occupancy of the cyclin D1 gene promoter. HeLa S3 cells expressing Flag-NOL1 (or empty vector) and hTERT shRNAs (or control shRNA) were cross-linked with formaldehyde, followed by immunoprecipitation with anti-Flag antibody. The immunoprecipitated chromatin was used as template to amplify the TBE in the cyclin D1 promoter. The primers used in PCR analysis was used for probing the presence of NOL1 and hTERT on the cyclin D1 promoter. The results showed that Flag-antibody immunoprecipitated the TBE-containing fragment when Flag-NOL1 was overexpressed (Fig. 6a). This TBE signal was not influenced by depletion of endogenous hTERT, suggesting that NOL1 binds to the TBE independently of hTERT. No amplification was observed when the immunoprecipitated chromatin was used to amplify the 3'-untranslated region (3'-UTR) (Fig. 6a). Because transcriptional activation by NOL1 is promoter-specific, we examined whether NOL1 is recruited to the c-Myc promoter and found that the Flag-NOL1 ChIP signal was not detected at the TBE of the c-Myc promoter, suggesting that NOL1 is not involved in the regulation of c-Myc transcription (Fig. 6b). We next analyzed the effect of hTERT depletion on the cyclin D1 transcription by luciferase assay. In HeLa S3 cells expressing the empty vector, depletion of hTERT reduced cyclin D1 promoter activity (Fig. 6c). However, in cells expressing Flag-NOL1, cyclin D1 promoter activity was hyperactivated by NOL1 overexpression, and which was not affected by depletion of hTERT, further supporting the idea that NOL1 activates the transcription of cyclin D1

independently of hTERT expression.

As we confirmed that NOL1 is independent of hTERT to bind to the cyclin D1 promoter, we tested whether occupancy of the cyclin D1 promoter by hTERT depends on NOL1, HeLa S3 cells expressing Flag-hTERT (or empty vector) and NOL1 shRNAs (or control shRNA) were subjected to ChIP. The results showed that Flag-hTERT associates with the TBE-containing fragment of the cyclin D1 promoter in cells expressing control shRNA (Fig. 6d). When endogenous NOL1 was depleted, the ability of Flag-hTERT to bind to the TBE fragment was abrogated. These results suggest that hTERT can be recruited to the cyclin D1 promoter through the interaction with NOL1. Intriguingly, consistent ChIP signal of Flag-hTERT was detected at the TBE fragment of the c-Myc promoter regardless of NOL1 expression, supporting the previous idea that NOL1 is not involved in the c-Myc gene regulation (Fig. 6e). We also examined the effect of NOL1 depletion on the cyclin D1 transcription. As expected, cyclin D1 promoter activity was downregulated by NOL1 depletion in HeLa S3 cells, (Fig. 6f). Even in the presence of overexpression of hTERT, cyclin D1 promoter activity could not be activated due to NOL1 depletion (Fig. 6f), suggesting that NOL1 is required for TERT to activate cyclin D1 transcription.

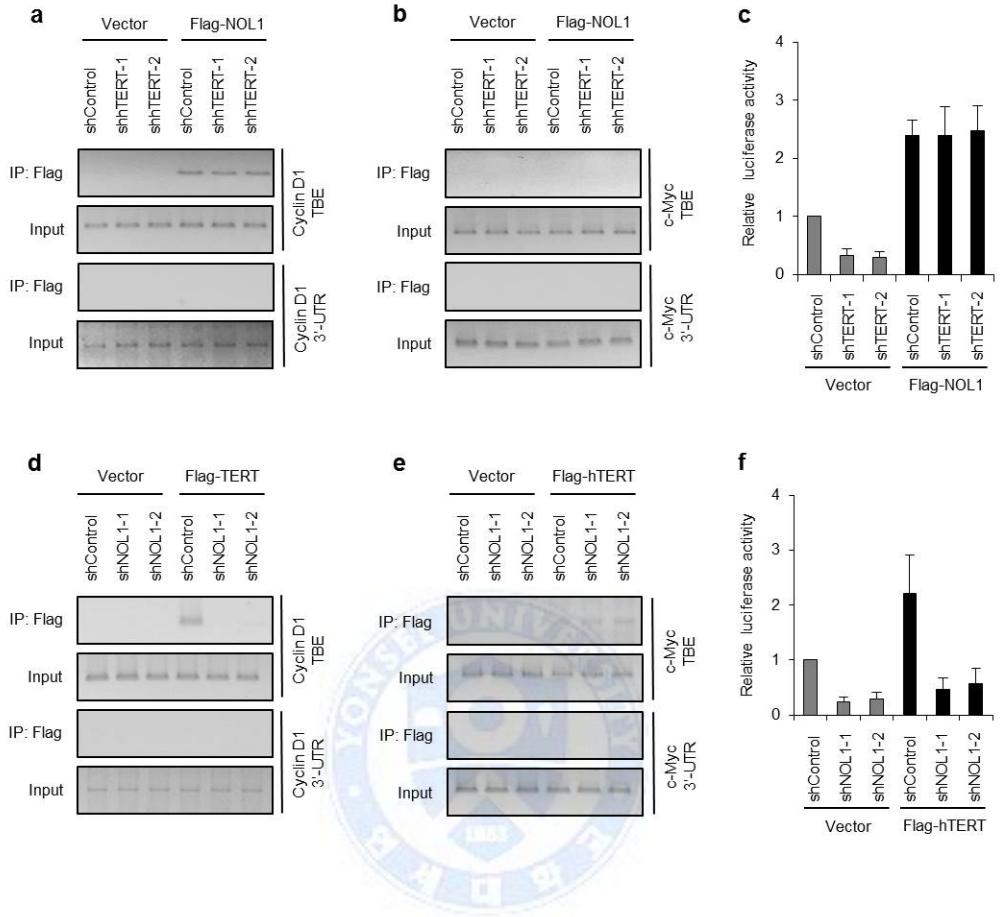

Figure 6. NOL1 and hTERT associate with the cyclin D1 promoter at the TBE. (a, b) HeLa S3 cells were transfected with Flag-NOL1 (or empty vector) together with hTERT shRNA (or control shRNA), and ChIP analyses were performed using Flag-antibody. The recruitment of NOL1 to the cyclin D1 TBE (a) or c-Myc TBE (b) was quantified by gel-based PCR assay. The 3'-untranslated region (3'-UTR) was used as a negative control. (c) The luciferase assay in HeLa S3 cells transfected with Flag-NOL1 (or empty vector) together with hTERT shRNA (or control shRNA). The firefly luciferase activity was normalized against the Renilla luciferase activity. Error bars show the standard deviation from the mean of three independent experiments. (d, e) HeLa S3 cells were transfected with Flag-hTERT (or empty

vector) together with NOL1 shRNA (or control shRNA), and ChIP analyses were performed using Flag-antibody. The recruitment of NOL1 to the cyclin D1 TBE (d) or c-Myc TBE (e) was quantified by gel-based PCR assay. The 3'-untranslated region (3'-UTR) was used as a negative control. (f) The luciferase assay in HeLa S3 cells transfected with Flag-hTERT (or empty vector) together with NOL1 shRNA (or control shRNA). The firefly luciferase activity was normalized against the Renilla luciferase activity. Error bars show the standard deviation from the mean of three independent experiments.

4.9 Depletion of NOL1 induces cell growth arrest.

Since cyclin D1 plays an important role in the cell cycle progression through G1 phase (Yu et al., 2001), we determined the effect of NOL1 depletion on cell growth. HeLa S3 cells were transduced with the retrovirus particles expressing the control shRNA or NOL1 shRNAs, and stable cell lines were established from separate transductions to monitor the population doubling (PD) levels at regular intervals. The control HeLa S3 cells grew normally and continued to divide throughout the duration of the experiments (Figure 7a). In contrast, the growth rates of two independent NOL1 knockdown cells (NOL1 shRNA-1 and NOL1 shRNA-2) gradually slowed down and stopped dividing at ~45 PD and ~30 PD, respectively. To determine whether the growth arrest correlates with an altered cell cycle distribution, the control cells and NOL1 knockdown cells were subjected to flow cytometric analysis by propidium iodide staining. At early PD, NOL1 knockdown cells showed cell cycle arrest at G1 phase compared with cells expressing control shRNA (Figure 7b). In addition, NOL1 knockdown cells exhibited a significant increase in sub-G1 DNA content at late PD, a characteristic of apoptosis (Figure 7c). Thus, the growth arrest of NOL1-knockdown cells could result from an inhibition of G1/S transition and an increased rate of cell death. Moreover, NOL1 knockdown cells showed increased levels of Bax and caspase-3 and decreased levels of Bcl-2 (Figure 7d). Taken together, these data support the idea that a growth arrest phenotype resulting from NOL1 depletion could be due to suppression of cyclin D1 transcription.

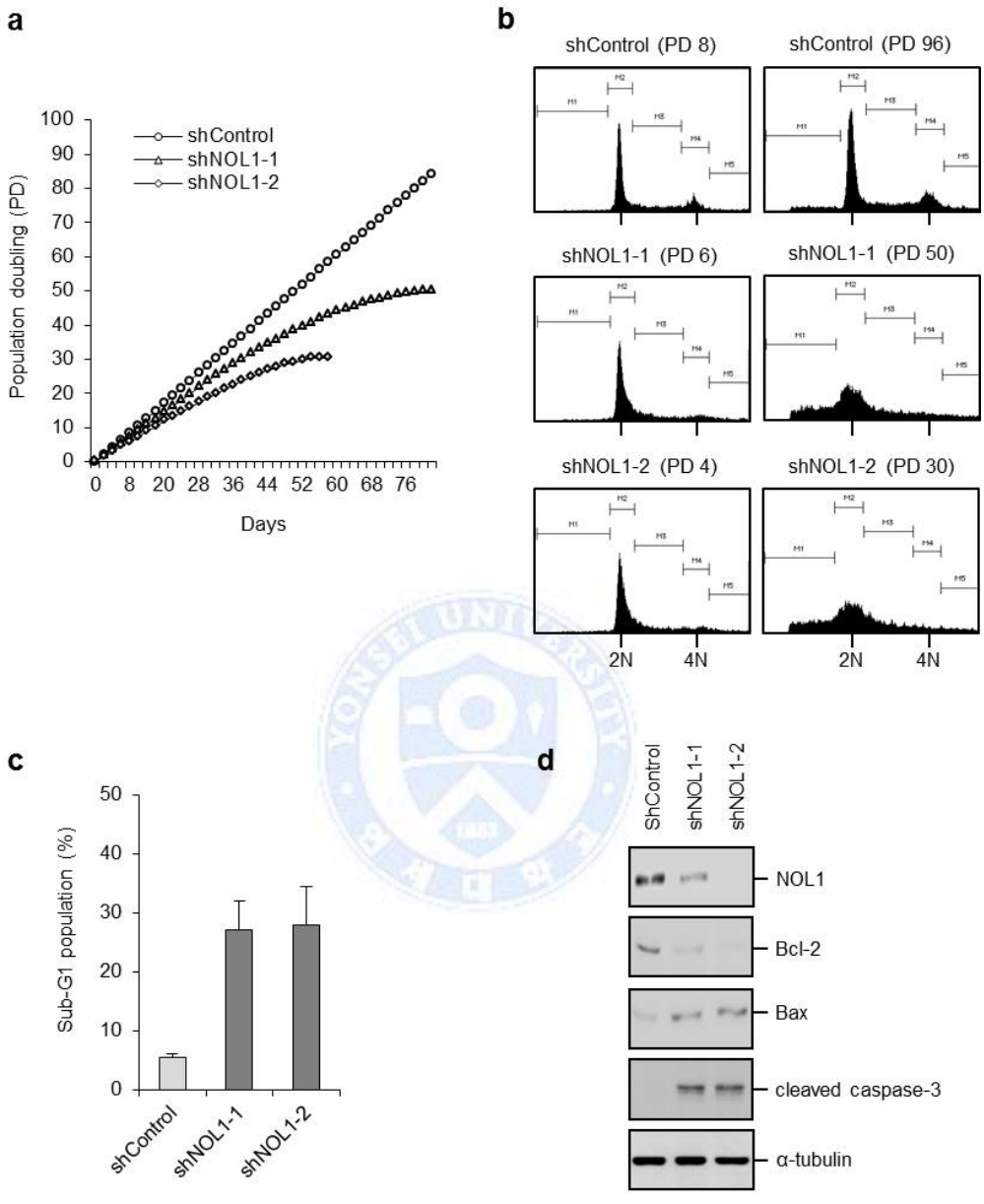

Figure 7. Depletion of NOL1 induces cell growth arrest. (a) Cell growth curves of HeLa S3 cells stably expressing control shRNA or NOL1 shRNAs. Cells were repeatedly transfected with KIP siRNAs at 3-day intervals for 15 days. HeLa S3 cells were infected with the retrovirus particles to establish stable cell lines. Stable cells were replated every 3-4 days to

maintain log-phase growth and calculate the growth rate, with day 0 representing the first day after puromycin selection. (b) Flow cytometric analysis of HeLa S3 cells stably expressing control shRNA or NOL1 shRNAs. Cells were stained with propidium iodide at early and late PDs, followed by FACS analysis. (c) The percentage of total cells in sub-G1 phase of the cell cycle is shown. (d) HeLa S3 cells stably expressing control shRNA or NOL1 shRNAs were analyzed by immunoblot to measure the protein levels of Bcl2, Bax and caspase-3.

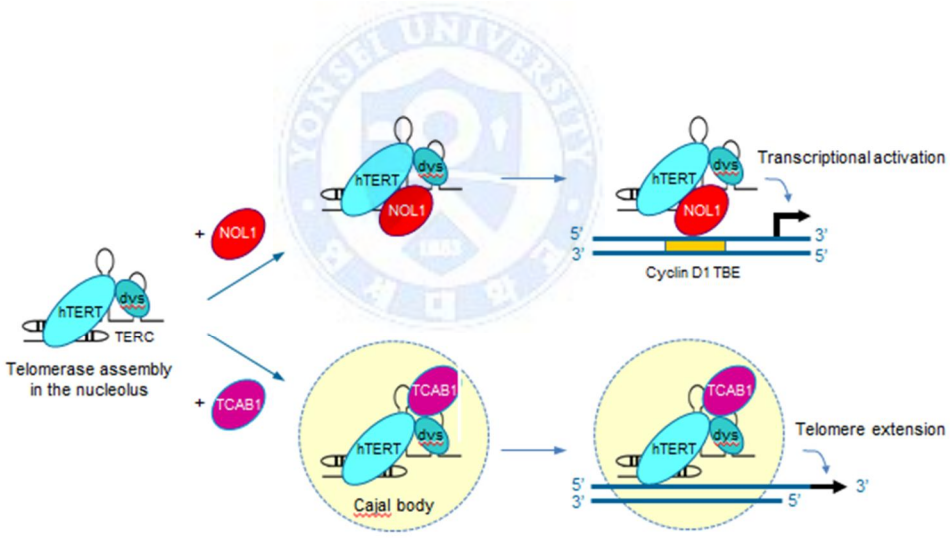

Figure 8. Proposed model for the two fates of telomerase during the assembly, telomere extension and transcriptional activation. After transcription, a TERC molecule assembles with dyskerin and hTERT in the nucleolus. Upon association with NOL1, the telomerase-NOL1 complex is recruited to the TBE of the cyclin D1 promoter and activates its

transcription. For telomere extension, telomerase associates with TCAB1 and is transported to Cajal bodies. Telomerase-containing Cajal bodies are loaded on telomeric chromatin to elongate telomere repeats. Because both NOL1 and TCAB1 associate with telomerase through TERC binding, these two factors might compete for binding to telomerase in the nucleolus.

5. Discussion

Various studies have shown that human telomerase is highly expressed in most maligmant tumors while it is hardly detectable in normal human somatic cells which have a limited proliferative lifespan and eventaully enter a nondividing state of replicative senescence[13]. Although ectopic expression of telomerase is sufficient to extend a lifespan, recent studies have suggested that the ability of telomerase to promote tumorigenesis requires additional activities that are independent of its role in telomere extension[14,15]. Here we identify NOL1 as a TERC-binding protein, which is found in association with catalytically active telomerase. Since NOL1 has no direct regulatory effect on the canonical function of telomerase including the assembly and trafficking of telomerase as well as its enzymatic activity, it is possible that NOL1 is involved in extra-telomeric function of telomerase. We discovered that NOL1 activates transcription of cyclin D1 gene by binding to the TCF binding element(TBE) of cyclin D1 promoter. Moreover, Telomerase is also recruited to the cyclin D1 promoter through the interaction with NOL1, further enhancing transcription of cyclin D1 gene. These data suggest that NOL1 represents a new pathway by which telomerase activates cyclin D1 transcription, thus bypassing cell cycle checkpoint signaling pathway and allowing cells keep proliferating.

In addition to its primary role in telomere elongation, it has been recently reported that telomerase has noncanonical functions in signaling pathways that influence human tumorigenesis[18,19,22]. Telomerase has been shown to bind to the NF-κB p65 subunit and localize to the promoters of a subset of NF-κB target genes[22]. Moreover, inhibition of telomerase reduced the expression of NF-κB-dependent genes, indicating that telomerase acts

as a transcriptional modulator of the NF-κB signaling cascade in cancer cells. Telomerase has also been found to act as a transcriptional modulator of Wnt/β-catenin signaling pathway through the interaction with BRG1, leading to enhanced expression of Wnt target genes such as cyclin D1 and c-MYC[19]. Furthermore, overexpression of alternatively spliced variants that lack telomerase activity stimulates cell proliferation by activating Wnt signaling[42]. However, an influence of hTERT as a transcriptional modulator on Wnt signaling has not been consistently reproduced[20,21]. The discrepancy in the effects of hTERT overexpression may be attributed to the different cell types and experimental conditions. Since Wnt signaling target genes are also regulated by other signaling pathways[43], the mechanism by which hTERT enhances the expression of growth-promoting genes could not be solely dependent on Wnt signaling. In this work, we show that telomerase interacts with NOL1 and promotes transcription of cyclin D1 gene in the absence of Wnt or NF-κB signaling. Whereas NOL1 alone is sufficient to bind to the cyclin D1 promoter and promote its transcription, hTERT is recruited to the cyclin D1 promoter through its interaction with NOL1, suggesting that telomerase activates cyclin D1 transcription in a NOL1-dependent manner. Although TERC is not required for telomerase-dependent transcriptional gene activation in Wnt/β-catenin signaling, it is essential for cyclin D1 activation by NOL1 and telomerase. Analysis of domain mapping revealed that TERC binding domain in hTERT is responsible for NOL1 binding. Furthermore, we found the direct NOL1 interaction with TERC, supporting that the association between NOL1 and hTERT is dependent on TERC. Thus, a functional interplay between NOL1 and telomerase modulates the prolonged expression of cyclin D1 gene which is critical for the maintenance of cell proliferation.

NOL1 is a proliferation-related nucleolar protein, which is highly expressed in most

malignant tumor cells but not in normal resting cells[23,24]. Since telomerase is initially assembled in the nucleolus[31], the finding that NOL1 is a novel component of catalytically active telomerase suggests that the nucleolus could be the site where NOL1 associates with the telomerase holoenzyme. Based on our data, we propose a model for the two fates of telomerase during its initial assembly, telomere extension and transcriptional activation (Fig. 8). The assembly of the active telomerase holoenzyme occurs in a highly elaborate, stepwise fashion31. After transcription, a TERC molecule assembles with a preformed dyskerin complex, and the subsequent assembly of TERC-dyskerin RNP with hTERT occurs specifically during the S phase in the nucleolus. For telomere extension, telomerase associates with TCAB1 and is transported to Cajal bodies[10,34]. Telomerase-containing Cajal bodies are loaded on telomeric chromatin to elongate telomere repeats. On the other hand, when NOL1 is recruited to the telomerase RNP in the nucleolus, the NOL1-telomerase complex binds to the cyclin D1 promoter at the TCF binding site. Since both TCAB1 and NOL1 associate with telomerase through the interaction with TERC, these two proteins might compete for binding to telomerase in the nucleolus. The outcome of this competition may likely determine which of the two fates of telomerase is favored. Although we cannot rule out the possibility that both proteins exist in the telomerase complex, it will be interesting to investigate what fractions of the telomerase RNP contain NOL1 or TCAB1.

NOL1 is known to be expressed early in the G1 phase and peaks during the S phase[25-27]. Thus, NOL1-dependent transcriptional activation of cyclin D1 gene may occur in a cell cycle-dependent manner. When telomerase is up-regulated in cancer cells, it could interact with NOL1 and occupy the TCF binding element of the cyclin D1 promoter to further facilitate the gene expression. Thus, NOL1 plays an important role in cell cycle progression through G1

phase and is implicated as a tumor cell marker. On the contrary, repressing the cyclin D1 expression by NOL1 depletion prevents the tumor cells exit from G1 phase, reversing tumor characters. Consistent with this idea, depletion of NOL1 induced a growth arrest at G1 phase in telomerase-positive HeLa S3 cells. This growth arrest was accompanied by several features consistent with the induction of apoptosis, including a substantial increase in sub-G1 DNA content. NOL1 knockdown cells exhibited an increase in the levels of pro-apoptotic Bax and cleaved caspase-3 and a decrease in the level of anti-apoptotic Bcl2. Given the importance of both telomerase and NOL1 in cancer progression, the functional interaction of telomerase and NOL1 plays an important role in the control of cell cycle progression through transcriptional induction of the cyclin D1 gene. Overall, our results provide for a novel function of NOL1 as an important regulator of cell cycle and proliferation as well as insight into the noncanonical mechanism by which telomerase promotes cell proliferation and inhibits cell growth arrest.

6. References

1. Blackburn, E. H. Switching and signaling at the telomere. Cell 106, 661-673 (2001).

2. Smogorzewska, A. & de Lange, T. Regulation of telomerase by telomeric proteins. Annu. Rev. Biochem. 73, 177-208 (2004).

3. Palm, W. & de Lange, T. How shelterin protects mammalian telomeres. Annu. Rev. Genet. 42, 301-334 (2008).

4. Sfeir, A. & de Lange, T. Removal of shelterin reveals the telomere end-protection problem. Science 336, 593-597 (2012).

5. Lingner, J., Cooper, J. P. & Cech, T. R. Telomerase and DNA end replication: no longer a lagging strand problem? Science 269, 1533-1534 (1995).

6. Blasco, M. A. et al. Telomere shortening and tumor formation by mouse cells lacking telomerase RNA. Cell 91, 25-34 (1997).

7. Autexier, C. & Lue, N.F. The structure and function of telomerase reverse transcriptase. Annu. Rev. Biochem. 75, 493-517 (2006).

8. Bianchi, A. & Shore, D. How telomerase reaches its end: mechanism of telomerase regulation by the telomeric complex. Mol. Cell 31, 153-165 (2008).

9. Egan, E.D. & Collins, K. Biogenesis of telomerase ribonucleoproteins. RNA 18, 1747-1759 (2012).

10. Venteicher, A. S. et al. A human telomerase holoenzyme protein required for Cajal body localization and telomere synthesis. Science 323, 644-648 (2009).

11. Venteicher, A. S., Meng, Z., Mason, P. J., Veenstra, T. D. & Artandi, S. E. Identification of ATPases pontin and reptin as telomerase components essential for holoenzyme assembly. Cell

132, 945-957 (2008).

12. Kim, N. W. et al. Specific association of human telomerase activity with immortal cells and cancer. Science 266, 2011-2015 (1994).

13. Bodnar, A. G. et al. Extension of life-span by introduction of telomerase into normal human cells. Science 279, 349-352 (1998).

14. Stewart, S. A. et al. Telomerase contributes to tumorigenesis by a telomere length-independent mechanism. Proc. Natl. Acad. Sci. USA 99, 12606-12611 (2002).

15. Li, Y. & Tergaonkar, V. Noncanonical functions of telomerase: implications in telomerase-targeted cancer therapies. Cancer Res. 74, 1639-1644 (2014).

16. Smith, L. L., Coller, H. A. & Roberts, J. M. Telomerase modulates expression of growth-controlling genes and enhances cell proliferation. Nat. Cell Biol. 5, 474-479 (2003).

17. Sarin, K. Y. et al. Conditional telomerase induction causes proliferation of hair follicle stem cells. Nature 436, 1048-1052 (2005).

18. Choi, J. et al. TERT promotes epithelial proliferation through transcriptional control of a Myc- and Wnt-related developmental program. PloS Genet. 4, e10 (2008).

19. Park, J. -I. et al. Telomerase modulates Wnt signalling by association with target gene chromatin. Nature 460, 66-72 (2009).

20. Listerman, I., Gazzaniga, F. S. & Blackburn, E. H. An investigation of the effects of the telomerase core protein TERT on Wnt signaling in human breast cancer cells. Mol. Cell. Biol. 34, 280-289 (2014).

21. Strong, M. A. et al. Phenotypes in mTERT+/- and mTERT-/- mice are due to short telomeres, not telomere-independent functions of telomerase reverse transcriptase. Mol. Cell. Biol. 31, 2369-2379 (2011).

22. Ghosh, A. et al. Telomerase directly regulates NF-kB-dependent transcription. Nat. Cell Biol. 14, 1270-1281 (2012).

23. Ochs, R. L., Reilly, M. T., Freeman, J. W. & Busch, H. Intranucleolar localization of human proliferating cell nucleolar antigen p120. Cancer Res. 48, 6523-6529 (1988).

24. Jhiang, S. M., Yaneva, M. & Busch, H. Expression of human proliferation-associated nucleolar antigen p120. Cell Growth Differ. 1, 319-324 (1990).

25. Fonagy, A., Swiderski, C., Dunn, M. & Freeman, J. W. Antisense-mediated specific inhibition of p120 protein expression prevents G1- to S-phase transition. Cancer Res. 52, 5250-5256 (1992).

26. Fonagy, A. et al. Cell cycle regulated expression of nucleolar antigen p120 in normal and transformed human fibroblasts. J. Cell Physiol. 154, 16-27 (1993).

27. Gorczyca, W., Bruno, S., Melamed, M. R. & Darzynkiewicz, Z. Cell cycle-related expression of p120 nucleolar antigen in normal human lymphocytes and in cells of HL-60 and MOLT-4 leukemic lines: effects of methotrexate, camptothecin, and teniposide. Cancer Res. 52, 3491-3494 (1992).

28. Jegou, T. et al. Dynamics of telomeres and promyelocytic leukemia nuclear bodies in a telomerase-negative human cell line. Mol. Biol. Cell 20, 2070-2082 (2009).

29. Koonin, E. V. Prediction of an rRNA methyltransferase domain in human tumor-specific nucleolar protein p120. Nucleic Acids Res. 22, 2476-2478 (1994).

30. Gustafson, W. C. et al. Nucleolar protein p120 contains an arginine-rich domain that binds to ribosomal RNA. Biochem. J. 331, 387-393 (1998).

31. Lee, J. H. et al. Catalytically active telomerase holoenzyme is assembled in the dense fibrillar component of the nucleolus during S phase. Histochem. Cell Biol. 141, 137-152

(2014).

32. Lee, J. H., Khadka, P., Baek, S. H. & Chung, I. K. CHIP promotes human telomerase reverse transcriptase degradation and negatively regulates telomerase activity. J. Biol. Chem. 285, 42033-42045 (2010).

33. Tomlinson, R. L., Ziegler, T. D., Supakorndej, T., Terns, R. M. & Terns, M. P. Cell cycle-regulated trafficking of human telomerase to telomeres. Mol. Biol. Cell 17, 955-965 (2006).

34. Venteicher, A. S. & Artandi, S. E. TCAB1: driving telomerase to Cajal bodies. Cell Cycle 8, 1329-1331 (2009).

35. Takai, H., Smogorzewska, A. & de Lange, T. DNA damage foci at dysfunctional telomeres. Curr. Biol. 13, 1549-1556 (2003).

36. d'Adda di Fagagna, F. et al. A DNA damage checkpoint response in telomere-initiated senescence. Nature 426, 194-198 (2003).

37. Perlaky, L. et al. Increased growth of NIH/3T3 cells by transfection with human p120 complementary DNA and inhibition by a p120 antisense construct. Cancer Res. 52, 428-436 (1992).

38. Musgrove, E. A., Caldon, C. E., Barraclough, J., Stone, A. & Sutherland, R. L. Cyclin D as a therapeutic target in cancer. Nat. Rev. Cancer 11, 558-72. (2011).

39. Sears, R. C. The life cycle of C-myc: from synthesis to degradation. Cell Cycle 3, 1133-1137 (2004).

40. Pestell, R. G. et al. The cyclins and cyclin-dependent kinase inhibitors in hormonal regulation of proliferation and differentiation. Endocr. Rev. 20, 501-534 (1999).

41. Yu, Q., Geng, Y. & Sicinski, P. Specific protection against breast cancers by cyclin D1 ablation. Nature 411, 1017-1021 (2001).

42. Hrdlicková, R., Nehyba, J. & Bose, H. R. Alternatively spliced telomerase reverse transcriptase variants lacking telomerase activity stimulate cell proliferation. Mol. Cell. Biol. 32, 4283-4296 (2012).

43. Guo, X. & Wang, X. F. Signaling cross-talk between TGF-beta/BMP and other pathways. Cell Res. 19, 71-88 (2009).

44. Lee, G. E. et al. DNA-protein kinase catalytic subunit-interacting protein KIP binds telomerase by interacting with human telomerase reverse transcriptase. J. Biol. Chem. 279, 34750-34755 (2004).

45. Kim, J. H., Kim, J. H., Lee, G. E., Lee, J. E. & Chung, I. K. Potent inhibition of human telomerase by nitrostyrene derivatives. Mol. Pharmacol. 63, 1117-1124 (2003).

46. Kim, N. W. & Wu, F. Advances in quantification and characterization of telomerase activity by the telomeric repeat amplification protocol (TRAP). Nucleic Acids Res. 25, 2595-2597 (1997).

47. Abreu, E., Terns, R. M. & Terns, M. P. Visualization of human telomerase localization by fluorescence microscopy techniques. Methods Mol. Biol. 735, 125-137 (2011).

48. van Steensel, B., Smogorzewska, A. & de Lange, T. TRF2 protects human telomeres from end-to-end fusions. Cell 92, 401-413 (1998).

49. de Lange T. How telomeres solve the end-protection problem. Sicence 326:948-952 (2009)

50. Eros Lazzerini Denchi & de Lange T. Protection of telomeres through independent control of ATM and ATR by TRF2 and POT1. Nature 448, 1068-1071 (2007)

Chapter 2

TINF2 mRNA degradation by HuR modulates telomere function

1. Abstract

Shortened telomeres and stabilization of ARF tumor suppressors are most characteristic properties during a replicative senescence. In primary cells, telomeres are gradually shortened via the incomplete DNA replication. At the same time, ARF tumor suppressors are controlled by post-transcriptional regulatory processes, notably mRNA turnover and translation. Such processes include RNA binding proteins (RBPs) that selectively control the expression of subsets of genes. HuR (human antigen R), which is a member of the elav/hu family, facilitates senescent process through stabilizing mRNA of the ARF tumor suppressor. However, the precise linkage between stabilization of ARF tumor suppressor by HuR and shorten telomeres during a replicative senescence is unknown. Here, we show that HuR represses TINF2 (TRF1-Interacting Nuclear Factor 2) through its 3'UTR, and stabilized TINF2 plays a role as driving force to be shorten telomeres during a replicative senescence. We found that loss of HuR induces stabilization of TINF2 mRNA, and stabilized TINF2 induces progressive telomere shortening. Furthermore, facilitated telomere shortening by stabilized TINF2 occurs prior to cell cycle arrest by stabilization of the ARF tumor suppressor. Our results demonstrate that progressive telomere shortening are concomitant to stabilization of the ARF tumor suppressor under orchestration of HuR during a replicative senescence.

2. Introduction

During cell division, eukaryotic telomeres gradually shorten due to the incomplete replication of linear chromosomes by DNA polymerase, which is known as the end-replication problem (Blackburn 2001; Bell and Dutta 2002). Compensation for telomere attrition by telomerase is essential to overcome the end replication problem in stem cells and in most of the cancer cells (Weinrich et al. 1997; Marcand et al. 2000; Collins 2006). Telomere structural maintenance is important for chromosome integrity and has been implicated in aging and cancer (Mitchell et al. 1999; Artandi and Attardi 2005; Blasco 2005; Artandi 2006; Deng et al. 2008). Telomeres are composed of duplex tandem TTAGGG repeats with 3′ single-stranded G overhang and shelterin, a six-subunit complex that is required for the end-protection of chromosome ends (de Lange 2005). Shelterin localizes to telomeres via the duplex tandem TTAGGG repeat binding proteins TRF1 and TRF2 containing a C-terminal myb DNA-binding domain and an internal TRFH (TRF2 homology) homodimerization domain. TINF2 directly interacts with TRF1 and TRF2, and it binds to TPP1 that in turn recruits the 3' single-stranded overhang binding protein POT1 (de Lange 2009). Although human RAP1 binds to TRF2 at telomeres, recent reports have shown that human RAP1 is not involved in telomere protection role (Kabir et al. 2014).

TINF2, a central component linking between TRF1 and TRF2, connects TPP1/POT1 to TRF1/TRF2 and contributes to telomere length regulation (Kim et al. 1999; Kim et al. 2004; Ye and de Lange 2004; Ye et al. 2004; O'Connor et al. 2006; Abreu et al. 2010; Takai et al. 2011; Frescas and de Lange 2014b). Depletion of TINF2 causes substantial telomere deprotection due to destabilization of the shelterin components and induction of telomere

dysfunction-induced foci (TIFs) (Yamada et al. 2002; Kim et al. 2004; Yang et al. 2011; Bhanot and Smith 2012). Interestingly, TINF2 has a critical role in high-order telomeric complex assembly (Ye et al. 2004; Kaminker et al. 2005; O'Connor et al. 2006; Kim et al. 2008). Increased levels of TINF2 lead to slight telomere shortening, preventing telomerase from elongating telomeres due to closed-state telomere structure (Kim et al. 2004). Mutations in *TINF2* have been related to genetic diseases with premature aging phenotypes and bone marrow failures such as *dyskeratosis congenita*, *ataxia-pancytopenia*, and *aplastic anemia* (Savage et al. 2008b; Savage et al. 2008a; Tsangaris et al. 2008; Walne et al. 2008; Du et al. 2009; Walne and Dokal 2009; Bessler et al. 2010; Sarper et al. 2010; Yamaguchi et al. 2010; Yang et al. 2011; Gleeson et al. 2012; Sasa et al. 2012; Fukuhara et al. 2013; Frescas and de Lange 2014a; Alder et al. 2015).

Recently, extra-telomeric functions of TRF1, TRF2, RAP1, and TINF2 among six core telomere proteins have been reported (Martinez and Blasco 2011). In particular, TINF2 was shown to localize to mitochondria (Chen et al. 2012; Sullivan et al. 2012). Reduced TINF2 by RNAi knockdown induced a decrease of several metabolites in the glycolytic pathway and inhibited reactive oxygen species (ROS) production and increased mitochondrial ATP synthesis and oxygen consumption in cancer cells, suggesting a link between telomeric proteins and mitochondrial metabolic pathway. However, although TINF2 participates in metabolic regulation in cancer cells, mitochondrial function of TINF2 in senescent cells is still unclear.

RNA-binding proteins (RBPs) are known as post-transcriptional regulators of gene expression, acting primarily through 5′ and 3′ untranslated regions (UTRs) of gene (Dynan and Tjian 1985; Moore 2005; Keene 2007; Lunde et al. 2007; Simone and Keene 2013;

Gerstberger et al. 2014). The RBP HuR (human antigen R, a member of the elav/hu family) regulates of stability of numerous target mRNAs and modulates the translation of mRNAs (Hinman and Lou 2008). Although HuR is predominantly localized in nucleus, its post-transcriptional actions are linked to its cytoplasmic localization and its interaction with target mRNAs (Hinman and Lou 2008; Kim and Gorospe 2008). Through RIP-ChIP (RBP immunoprecipitation and microarray analysis) analysis or PAR-CLIP (Photoactivatable - Ribonucleoside-Enhanced Cross-linking and Immunoprecipitation) analysis, numerous functional mRNA targets directly bound to HuR were identified (Keene et al. 2006; Lebedeva et al. 2011). Moreover, AU-rich elements (AREs) and polypyrimidine motifs were identified with already known HuR binding motifs (UUUUUUU, UUUAUUU and UUUGUUU) within target mRNAs. Through its actions on target mRNAs, HuR has been implicated in various biological processes, including cell division, immune and stress responses, differentiation, and carcinogenesis (Wang et al. 2000a; Wang et al. 2000b; Dean et al. 2001; Wang et al. 2001; Figueroa et al. 2003; Gorospe 2003; Lopez de Silanes et al. 2003; Mazan-Mamczarz et al. 2003; Saunus et al. 2008; Ghosh et al. 2009; Katsanou et al. 2009; Kim et al. 2009; Topisirovic et al. 2009; Yi et al. 2010; Durie et al. 2011; Paukku et al. 2012; Srikantan et al. 2012; Durie et al. 2013; Kawagishi et al. 2013; Pang et al. 2013; Singh et al. 2013; Hashimoto et al. 2014; Liu et al. 2014; Diaz-Munoz et al. 2015; Kim et al. 2015). In particular, reduced levels of HuR are known to facilitate senescent process through stabilizing mRNA of the ARF tumor suppressor (Wang et al. 2001; Wang et al. 2003; Yi et al. 2010; Pang et al. 2013; Hashimoto et al. 2014). However, it remains unclear whether HuR-dependent senescent process is accompanied by telomere shortening, which is general phenomenon in senescent cells.

In this work, we demonstrate that HuR interacts with and destabilizes TINF2 mRNA through its 3' UTR. We found that functional activity and protein level of HuR are decreased, and which stabilizes TINF2 mRNA in senescent cells. We also show that knockdown of HuR by expressing retroviral shRNA induces telomere dysfunction-induced foci (TIFs) and cellular senescence, which is accompanied by G1 arrest in cancer cells. Furthermore, enhanced levels of TINF2 by knockdown of HuR led to substantial telomere shortening. Taken together, progressive telomere shortening due to enhanced levels of TINF2 by reduced level of HuR facilitates a replicative senescence with stabilization of the ARF tumor suppressor, suggesting that HuR orchestrates functional linkage between stabilization of ARF tumor suppressor and telomere shortening during a replicative senescence.

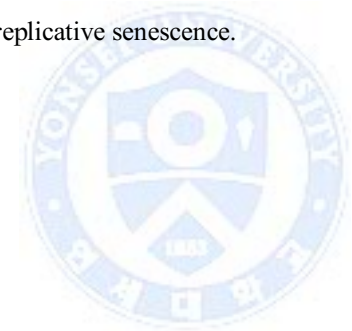

3. Materials and methods

Cell culture

Human cervical carcinoma HeLa S3 and HeLa CCL2 cells and human embryonic kidney HEK293 cells were grown in Dulbecco's modified Eagle's medium containing 10% fetal bovine serum with 100 units/mL penicillin, and 100 μg/mL streptomycin in 5% CO2 at 37 °C. Human osteosarcoma U2OS cells were grown in McCoy's modified medium with10% fetal bovine serum, 100 units/mL penicillin, and 100 μg/mL streptomycin in 5% CO2 at 37 °C.

Constructs

Standard recombinant DNA techniques were used to construct the following plasmids: FLAG-tagged HuR fragment in pLNCX2 plasmid (Clontech), GFP-TINF2 3'UTR chimeric fragments in pEGFP-C1 plasmid (Clontech). The expression vectors were transiently transfected using Lipofectamine 2000 reagent according to the manufacturer's protocol (Invitrogen).

Stable cell line generation using retroviral expressing vector.

293T cultures were grown in DMEM/10% bovine growth serum/100 units/mL penicillin, and 100 μg/mL streptomycin. Retroviruses were generated from 293T cells by cotransfecting plasmids encoding pGP (gag/pol; TAKARA), pE-ampho (env;TAKARA) and the retroviral shRNA plasmids by Lipofectamine 2000 (invitrogen). To generate stable cell lines, HeLa S3 cells were transduced with shRNA constructs in the pSUPER.retro.puro vector (Oligoengine), selected with 1μg/ml puromycin (GIBCO) for 2 weeks. For shRNA vectors, hairpin sequences

were:

shHuR-1: 5’-gatccccgtctgttcagcagcattggttcaagagaccaatgctgctgaacagacttttta-3’;

shHuR-2: 5’-gatcccctgtgaaagtgattcgtgatttcaagagaatcacgaatcactttcacattttta-3’

Semi-quantitative RT-PCR

Total RNA was isolated from HeLa S3 cells using Easy-BLUE (Intron, Korea). cDNA was reverse-transcribed from 1 μg of total RNA using M-MLV Reverse-Transcriptase (Promega) and used for semi-quantitative RT-PCR. For semi-quantitative PCR of mRNA following RNA-immunoprecipitation, the eluted immunoprecipitates were incubated with proteinase K at 45°C for 1hr, and then directly used for reverse transcription using the M-MLV reverse transcriptase. The following primers were used:

HuR F: 5'-CGC AGA GAT TCA GGT TCT CC-3’

HuR R: 5’-CCA AAC CCT TTG CAC TTG TT-3’

GFP F: 5'-TAA ACG GCC ACA AGT TCA GCG T-3’

GFP R: 5’-AAG TCG TGC TGC TTC ATG TGG T -3’

TRF1 F: 5'-GGC TGG ATG CTC GAT TTC CT-3’

TRF1 R: 5’-GCC GCT GCC TTC ATT AGA A-3’

TRF2 F: 5'-CAA GTT CTA CTT CCA CGA GGC G-3’

TRF2 R: 5’-GCG GAC TCA GAT TTC AAA GCC-3’

RAP1 F: 5'-GCC TTG TGG AAA GCG A-3’

RAP1 R: 5’-TCT GGA GTT CTC TTA TTC TGT-3’

POT1 F: 5'-TCC AGA TTC CAG CAT CAG A-3’

POT1 R: 5’-GCA TTC CAA CCA CGG ATA-3’

TPP1 F: 5'-GCT CAA TGC TGT GCA TCT CT-3’

TPP1 R: 5’-TGA GGA AGG AGG AGA GGC TA-3’

TINF2 F: 5'-TGT GGA TTT GGC CTC G-3’

TINF2 R: 5’-GAG AAG AGG TGA TAG AGA CT-3’

TERT F: 5'-CGG AAG AGT GTC TGG AGC AA-3’

TERT R: 5’-GGA TGA AGC GGA GTC TGG A-3’

TERC F: 5'-TCT AAC CCT AAC TGA GAA GGG CGT AG-3’

TERC R: 5'-GTT TGC TCT AGA ATG AAC GGT GGA AG-3’

dykerin F: 5'-ACA GGG TGA AGA GTT CTG GCA CAT-3’

dykerin R: 5'-TGA AGG TGA GGC TTC CCA ACT CAA-3’

TCAB1 F: 5'-CCA GCT CTT CTG TGG CTT CAA C-3’

TCAB1 R: 5'-AGG CTA TGC AGG AGA TGA TGC C -3’

SRSF11 F: 5'-TCC AGA CTC AGC AGT TGT GGC A -3’

SRSF11 R: 5'-GCA TTA GCT GGT GCC AAC AGA G -3’

GAPDH F: 5'-CTC AGA CAC CAT GGG GAA GGT GA-3’

GAPDH R: 5'-ATG ATC TTG AGG CTG TTG TCA TA -3’

Immunoprecipitation and immunoblot.

The following antibodies were used: anti-Flag (M2, Sigma), HuR (3A2, SantaCruz), GFP (B-2, SantaCruz), dyskerin (H-300, SantaCruz), TRF1 (C-19, SantaCruz), TRF2 (D1Y5D, Cell signaling), RAP1 (A300-306A, Bethyl laboratories), POT1 (ab21382, abcam), TPP1 (ab54685, abcam), TINF2 (ab136997, abcam), Lamin A/C (N-18, SantaCruz), p53 (FL-393, SantaCruz), p21 (C-19, SantaCruz), p16 (H-43, SantaCruz) and tubulin (TU-02, SantaCruz). For

immunoblotting, whole-cell lysates were prepared using NP-40 lysis buffer (0.5% NP-40, 1.5mM MgCl2, 25mM HEPES-KOH (pH7.5), 150mM KCl, 10% glycerol, Phosphotase inhibitor cocktail (Roche) and Proteinase inhibitor cocktail (Roche)) for 15 min at 4°C, followed by centrifugation (16,000 x g, 10 min). Supernatant fractions were denatured with 5X SDS sample buffer at 95°C for 7 min, fractionated by SDS–PAGE and transferred onto nitrocellulose membrane. For immunoblot blocking and antibody incubation, 5% non-fat dry milk in TBS-T (25mM Tris-HCl, pH 8.0, 125mM NaCl, 0.5% Tween-20) was used. And then, membranes were washed 3 times for 5 min each in TBS-T, incubated for 1 hr in peroxidase-conjugated secondary antibody (1:10,000, Gendepot), washed 3 times for 5 min each in TBS-T and developed with ECL (Santa Cruz) solution.

For immunoprecipitation, the cells were lysed with NP-40 lysis buffer for 15 min at 4°C, followed by spinning at 16,000 x g for 10 min. The cell lysates were pre-cleared with either mouse or rabbit IgG (SantaCruz) for 30 min and 30 μl of protein A sepharose (GE Healthcare). After spinning down (9,000 r.p.m., 1 min), the supernatant was transferred into fresh tubes and incubated with antibodies at 4°C overnight. Subsequently, 40 μl of protein A sepharose was added and incubated for 1 h. Immunoprecipitates were washed with NP-40 lysis buffer, then eluted by boiling in loading buffer and analysed by immunoblotting. Primary antibodies were used at the following concentrations: Flag (sigma): 500 ng/mL; HuR (SantaCruz): 200 ng/mL; GFP (SantaCruz): 200 ng/mL; dyskerin (SantaCruz): 200 ng/mL; TRF1 (SantaCruz): 200 ng/mL ; TRF1 (Cell signaling): 100 ng/mL; RAP1 (SantaCruz): 50 ng/mL; POT1 (abcam): 400 ng/mL; TPP1 (abcam): 200 ng/mL; TINF2 (abcam): 400 ng/mL; Lamin A/C (SantaCruz): 200 ng/mL; p53 (SantaCruz): 200 ng/mL; p21 (SantaCruz): 200 ng/mL; p16 (SantaCruz): 200 ng/mL; α-tubulin (SantaCruz): 200 ng/mL.

Immunofluorescence and Fluorescence in situ hybridization (FISH)

Cells grown on cover slips were fixed with 4% paraformadehyde in PBS for 10 min and permeabilized in PBS containing 0.5% Triton X-100 for 10 min. Afterwards, cells were blocked in PBG (PBS containing 0.5% BSA and 0.2% cold fish gelatin) for 10 min. Cells were incubated for 16 hr in PBG at 4°C with the following antibodies: anti-53BP1 (2μg/mL, sc-22760, SantaCruz), anti-γH2AX (2μg/mL, 2577, Cell signaling). Coverslips were washed 3 times with PBG for 5 min each followed by incubation with Alexa Fluor 488 goat anti-rabbit immunoglobulin and Alexa Fluor 568 goat anti-mouse immunoglobulin (Molecular Probes) for 1 hr in PBG at room temperature. Finally, cover slips were washed 3 times with PBG for 5 min each and mounted using VectaShield (H-1200, DAPI containing, Vector Labs) medium.
For PNA-FISH, Cells grown on cover slips were fixed with 4% paraformadehyde in PBS for 10 min and permeabilized in PBS containing 0.5% Triton X-100 for 10 min. Afterwards, cells were blocked in PBG (PBS containing 0.5% BSA and 0.2% cold fish gelatin) for 10 min. Cells were incubated for 16 hr in PBG at 4°C with primary anti-bodies. After PBS washes, coverslips were incubated with alexa 456 secondary antibody raised against mouse or rabbit for 45 min and washed in PBS. At this point, coverslips were fixed with 4% paraformaldehyde for 10 min at RT; washed extensively in PBS; dehydrated consecutively in 70%, 90%, and 100% ethanol for 5 min each; and allowed to dry completely. Hybridization solution (70% formamide, 1mg/ml blocking reagent [Roche], 10Mm Tris-HCl, pH 7.2), containing the peptide nucleic acid(PNA) probe fluorescein isothiocyanate (FITC)-OO-(CCCTAA)3(Applied Biosystems), was added to each coverslip, and the cells were denatured by heating for 10 min at 82°C on a heat block. After 12-14 hr incubation at RT in the dark, cells were washed twice with washing solution (70% formamide, 10mm Tris-HCl, pH7.2) and twice in PBS. DNA was

counterstained with DAPI (4',6-diamidino-2-phenylindole) and the images were analyzed by Confocal microscopy analysis.

Fluorescence-activated Cell Sorter (FACS) Analysis

HeLa S3 cells were washed with ice-cold PBS and fixed for 30 min in ice-cold serially diluted 70% ethanol. The fixed cells were resuspended in PBS containing RNase A (200 μg/ml) and propidium iodide (50 μg/ml) and incubated in the dark for 30 min at room temperature. Cell cycle progression was monitored by flow cytometry using a FACScan flow cytometer (BD Biosciences).

Double thymidine block of HeLa S3 cells

HeLa S3 cells were grown in Dulbecco's modified Eagle's medium (Hyclone) containing 10% fetal bovine serum (Hyclone). Cells in the logarithmic growth phase were incubated in medium containing 5 mM thymidine (Sigma). After 19 hrs, cells were washed twice with PBS and grown in regular medium for 9 hrs before a second incubation with 2 mM thymidine for 18 hrs. Cells released from the second thymidine block were collected at 2 hr intervals.

4. Results

4.1 HuR associates with TINF2 mRNA.

HuR contains three RNA recognition motifs (RRMs) for binding to 5′ and 3′ untranslated regions (UTRs) of target mRNAs (Keene 2007; Wang et al. 2011; Simone and Keene 2013; Wang et al. 2013). Ribonucleoprotein (RNP) associations comprising (Peng et al. 1998; Lebedeva et al. 2011) HuR and its target mRNAs are controlled by proliferative and damage signals. Given the functions of its target mRNAs, HuR has been implicated in processes such as cellular proliferation, cellular senescence and responses to DNA damage (Wang et al. 2000a; Wang et al. 2000b; Wang et al. 2001; Mazan-Mamczarz et al. 2003; Wang et al. 2003; Kim et al. 2010; Yi et al. 2010; Pang et al. 2013; Hashimoto et al. 2014; Lal et al. 2014). Thus, we suggested that HuR has functional relationship with shelterin components. To determine whether HuR associates with mRNA of shelterin components, we first performed cross-linked immunoprecipitation (CLIP)-PCR assays in HeLa S3 cells or U2-OS cells (Figure 1). After UV cross-linking, endogenous HuRs were immunprecipitated with HuR-specific antibody and eluted mRNAs were analyzed by the semi-quantitative reverse-transcription (RT)-PCR (Figure 1). The results showed that endogenous HuR associates with mRNA of TINF2 only (Figure 1A and B). We also investigated functional relationship between HuR and mRNA of telomerase holoenzyme components (TERT, TERC, dyskerin, TCAB1, SRSF11). We found that mRNA of telomerase holoenzyme components do not associate with HuR (Figure 1A). Moreover, in U2-OS cells, which are telomerase negative cells, our results showed that endogenous HuR associates with mRNA of TINF2 only (Figure 1B). Taken together, HuR

associates with mRNA of TINF2 in both telomerase positive- and negative cancer cells.

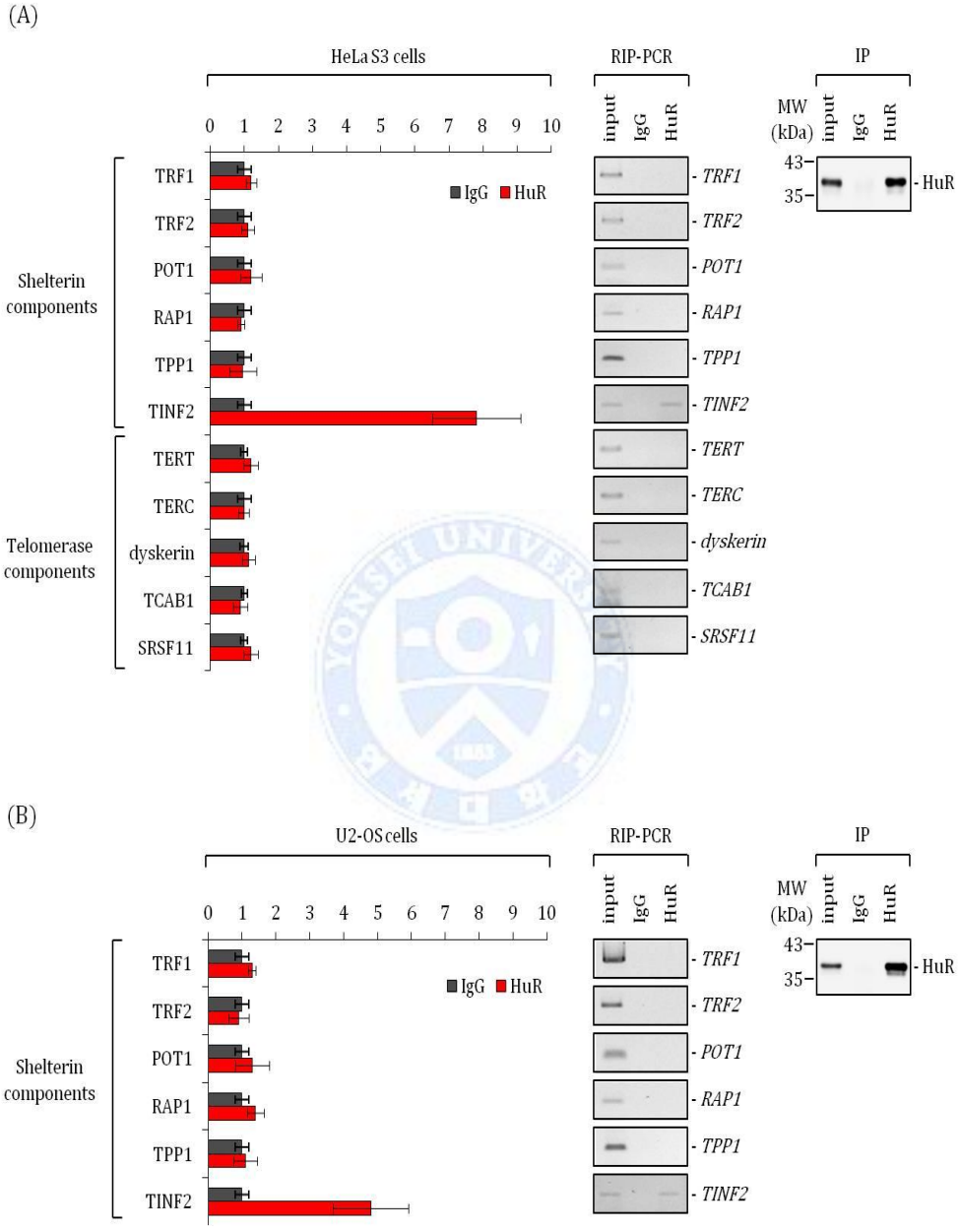

Figure. 1. HuR associates with *TINF2* mRNA

Figure. 1. HuR associates with TINF2 mRNA (A) HeLa S3 cell lysates were subjected to RNP IP followed by RT–PCR analysis to measure the enrichment of shelterin mRNAs in HuR IP compared with control IgG IP. Graphical representation of the relative levels of shelterin mRNAs in HuR IP normalized against IgG IP. The mRNA levels were quantified with the average and standard deviation from three independent experiments. (B) U2-OS cell lysates were subjected to RNP IP followed by RT–PCR analysis to measure the enrichment of shelterin mRNAs in HuR IP compared with control IgG IP. Graphical representation of the relative levels of shelterin mRNAs in HuR IP normalized against IgG IP. The mRNA levels were quantified with the average and standard deviation from three independent experiments.

4.2. HuR does not associate with shelterin components and telomerase components in protein level.

HuR function in telomere is implicated in the regulation related to TERRA, which is a non-coding RNA (Lopez de Silanes et al. 2010). Most of RNA regulation by HuR occurs at post-transcriptional level. To exclude functional relationship between HuR and shelterin components/telomerase components in protein level, we performed co-immunoprecipitation (co-IP) assays. First, Flag-tagged shelterin components (TRF1, TRF2, RAP1, POT1, TPP1, TINF2) were transfected to HEK293cells and were immunoprecipitated with Flag M2-resin. The results show that shelterin components did not interact with HuR (Figure 2A). Moreover, in co-IP experiment with active telomerase components (TERT, dyskerin, TCAB1, SRSF11), they did not interact with HuR (Figure 2B).

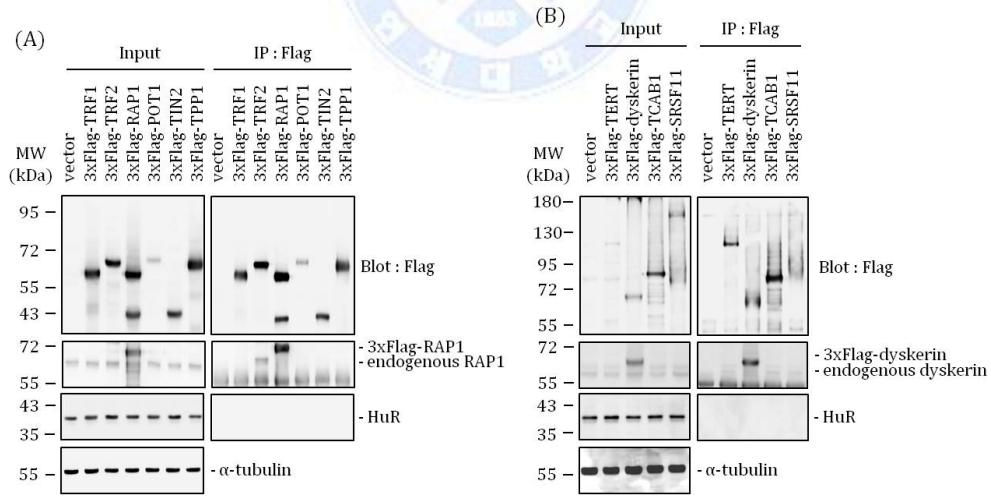

Figure 2.HuR does not associate with shelterin components and telomerase components at protein level.

Figure 2.HuR does not associate with shelterin components and telomerase components at protein level. (A) Lysates from HEK293 cells expressing Flag-TRF1, Flag-TRF2, Flag-RAP1, Flag-POT1, Flag-TPP1 or Flag-TINF2 were immunoprecipitated with anti-Flag antibody, followed by immunoblotting with anti-Flag, anti-HuR and anti-α-tubulin antibodies. (B) Lysates from HEK293 cells expressing Flag-TERT, Flag-dyskerin, Flag-TCAB1 or Flag-SRSF11 were immunoprecipitated with anti-Flag antibody, followed by immunoblotting with anti-Flag, anti-HuR and anti-α-tubulin antibodies.

4.3. HuR represses TINF2 expression at post-transcriptional level.

HuR is known as a modulator to regulate mature mRNA stability and translation. Thus, we suggested that HuR regulates TINF2 expression in vivo. To investigate whether HuR affects shelterin components at post-transcriptional level and translational level, we analyzed the expression level of shelterin components by overexpression of HuR. We first transduced retroviral pLNCX2-vector and pLNCX2-3xFlag-HuR to HeLa S3 cells (Figure 3). After incubation for 36hrs, cells were analyzed by Western blot assay with specific antibodies. The results showed that the overexpression of HuR reduced TINF2 protein level only (Figure 3A and B). Furthermore, we performed semi-quantitative RT-PCR assay to compare mRNA level of shelterin components by HuR. Consistent with the effect on protein level, overexpression of HuR reduced TINF2 mRNA only (Figure 3C and D). To further confirm that HuR negatively reduces TINF2 expression at post-transcriptional level, we transduced retroviral pLNCX2-vector and pLNCX2-3xFlag-HuR to HeLa S3 cells and treated MG132 (proteasome inhibitor) for 4hrs before harvesting cells (Figure 3E and F). The results showed that HuR substantially decreased TINF2 expression at protein level and the reduced TINF2 levels were not recovered by treatment of MG132, indicating that HuR represses TINF2 expression at post-transcriptional level.

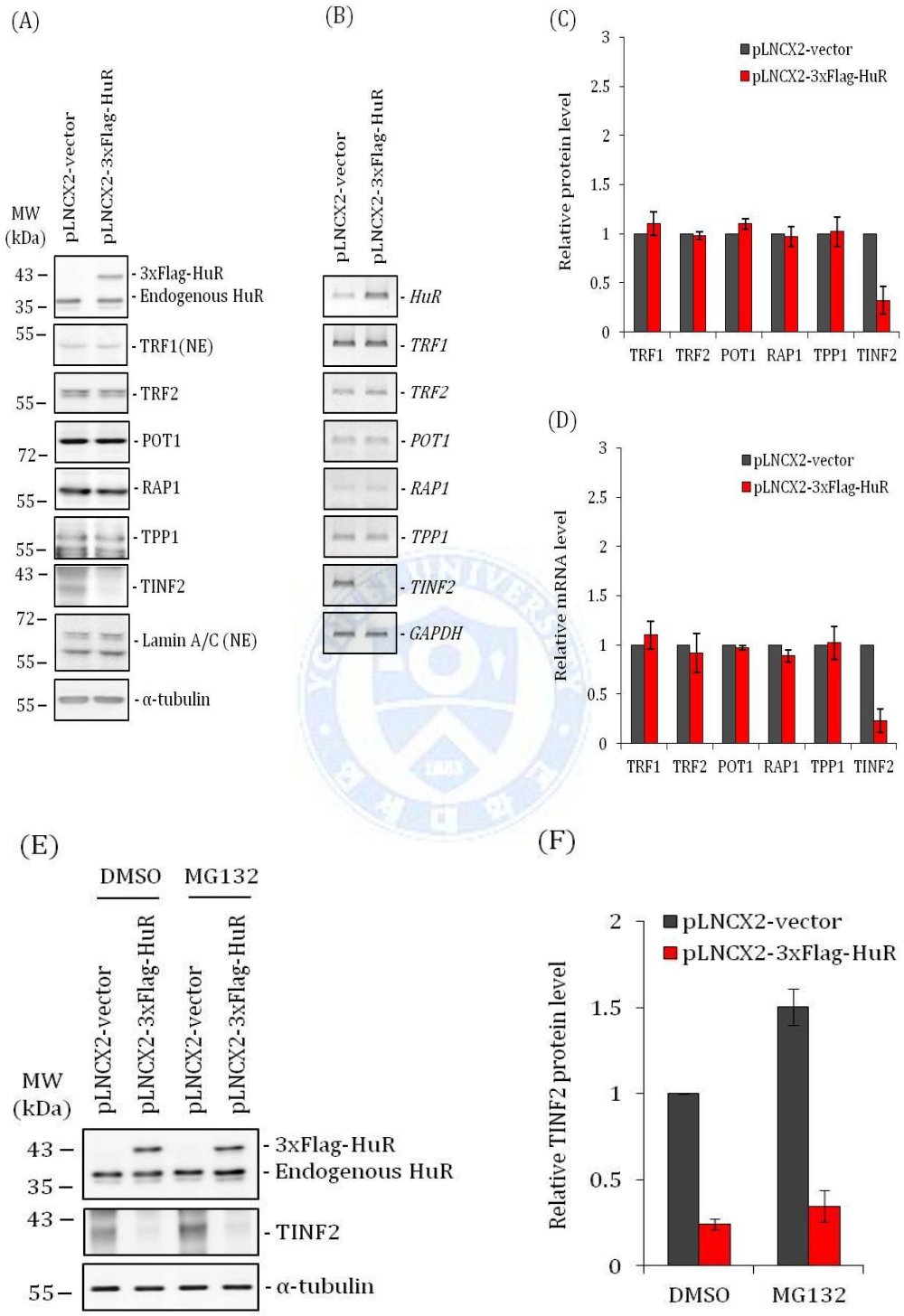

Figure 3. HuR represses TINF2 expression at post-transcriptional level.

Figure 3.HuR represses TINF2 expression at post-transcriptional level. (A) Forty-eight hours after transduction with a control plasmid expressing pLNCX2-vector or a plasmid overexpressing HuR as tagging protein 3xFlag-HuR in HeLa S3 cells, the levels of endogenous HuR, 3xFlag-HuR, TRF1(NE), TRF2, RAP1, POT1, TPP1, TINF2, Lamin A/C (NE) and α-tubulin were measured by the indicated antibodies. Graphical representation of the relative levels of shelterin proteins in overexpressed HuR normalized against a control in (C). The protein levels were quantified with the average and standard deviation from three independent experiments. NE; nuclear extracts. (B) Forty-eight hours after transduction with a control plasmid expressing pLNCX2-vector or a plasmid overexpressing HuR as tagging protein 3xFlag-HuR in HeLa S3 cells, HuR, TRF1, TRF2, RAP1, POT1, TPP1, TINF2 and GAPDH were measured by RT-PCR. Graphical representation of the relative levels of shelterin mRNA in overexpressed HuR normalized against a control in (D). The mRNA levels were quantified with the average and standard deviation from three independent experiments. (E) Forty-eight hours after transduction with a control plasmid expressing pLNCX2-vector or a plasmid overexpressing HuR as tagging protein 3xFlag-HuR in HeLa S3 cells, DMSO or 10μM MG132 (proteasome inhibitor) were treated for 6hrs. The levels of endogenous HuR, 3xFlag-HuR, TINF2 and α-tubulin were measured by the indicated antibodies. Graphical representation of the relative levels of TINF2 in overexpressed HuR normalized against a control in the absence (DMSO) or presence of MG132 in (F).

4.4. HuR does not affect TINF2 protein stability.

HuR affects translational efficiency of mRNA and stability of proteins (eg. P53, XIAP, Wnt-5a and HMGB1 etc.) (Mazan-Mamczarz et al. 2003; Leandersson et al. 2006; Durie et al. 2011; Dormoy-Raclet et al. 2013). To determine whether HuR affects protein stability of TINF2, we performed protein degradation assay with treatment of cycloheximide (protein de novo synthesis inhibitor). For knockdown of endogenous HuR, We first transduced retroviral shvector, shHuR-1 and shHuR-2 to HeLa S3 cells. After incubation of 36hrs, knockdown efficiency of HuR was analyzed by Western blot assay with specific HuR antibody (not shown in here). Harvested cells were subjected to Western blot assay with specific TINF2 antibody. The results showed that depletion of HuR did not affect protein stability of TINF2 (Figure 4A and B). Conversely, we transduced retroviral pLNCX2-vector and pLNCX2-3xFlag-HuR to HeLa S3 cells. The results showed that HuR represses TINF2 protein expression level, but does not affect protein stability of TINF2 (Figure 4C and D). Taken together, intrinsic TINF2 protein itself is not regulated by HuR.

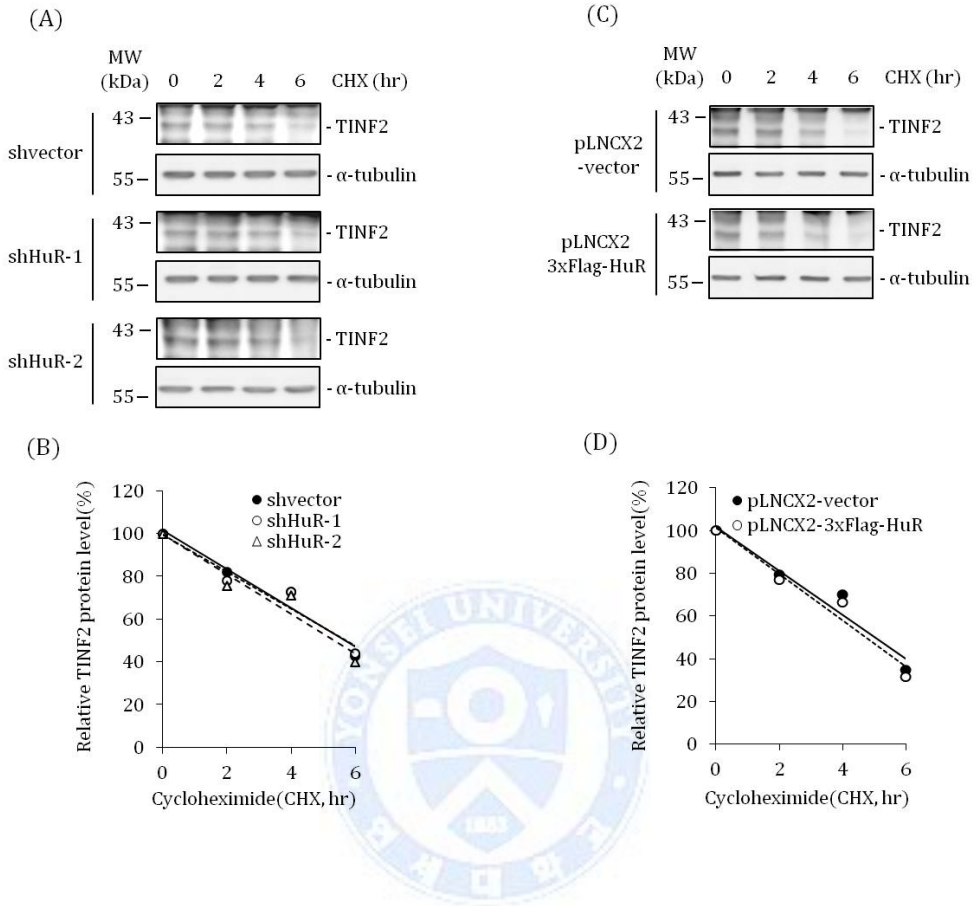

Figure 4. HuR does not affect TINF2 protein stability. (A) Forty-eight hours after transduction with shvector or HuR shRNAs in HeLa S3 cells, cells were treated with cycloheximide (CHX, 10 mg/ml) and the levels of TINF2 and loading control α-tubulin were assessed by Western blot analysis. Graphical representation of the relative levels of TINF2 proteins normalized against α-tubulin in (B). The protein levels were quantified with the average and standard deviation from three independent experiments. (C) Forty-eight hours after transduction with pLNCX2-vector or a plasmid overexpressing HuR as tagging protein 3xFlag-HuR in HeLa S3 cells, cells were treated with cycloheximide (CHX, 10 mg/ml) and the levels of TINF2 and loading control α-tubulin were assessed by Western blot analysis.

Graphical representation of the relative levels of TINF2 proteins normalized against α-tubulin in (D). The protein levels were quantified with the average and standard deviation from three independent experiments.

4.5. HuR regulates TINF2 expression through the TINF2 3'UTR.

To investigate whether HuR influences TINF2 expression by acting on the TINF2 3´UTR, a heterologous reporter construct expressing a chimeric RNA that spanned the GFP CR and the TINF2 3´UTR (Figure 5) was tested. As shown, overexpression of HuR reduced the expression level of GFP (Figure 5A) from the reporter chimeric plasmid pGFP(3´UTR), but not from pGFP. Graphical representation of the relative levels of GFP proteins normalized against α-tubulin was shown in Figure 5B. To further confirm the reduced expression of GFP-3'UTR, we performed semi-quantitative RT-PCR with same experimental conditions. The results showed that overexpression of HuR reduced the expression of GFP-3'UTR at post-transcriptional level (Figure 5A). Graphical representation of the relative levels of GFP mRNA normalized against GAPDH was shown in Figure 5C. Conversely, we tested whether HuR silencing influences TINF2 expression. We cotransfected shvector or shHuR with reporter chimeric plasmids to HeLa CCL2 cells. As shown in figure 5D-F, knockdown of HuR enhanced the expression of GFP-3'UTR (Figure 5D). Graphical representation of the relative levels of GFP proteins normalized against α-tubulin was shown in Figure 5E. The enhanced expression of TINF2 was also confirmed by semi-quantitative RT-PCR with same experimental condition (Figure 5D). Graphical representation of the relative levels of GFP mRNA normalized against GAPDH was shown in Figure 4F. Taken together, we suggest that HuR represses TINF2 expression through 3'UTR of TINF2 mRNA.

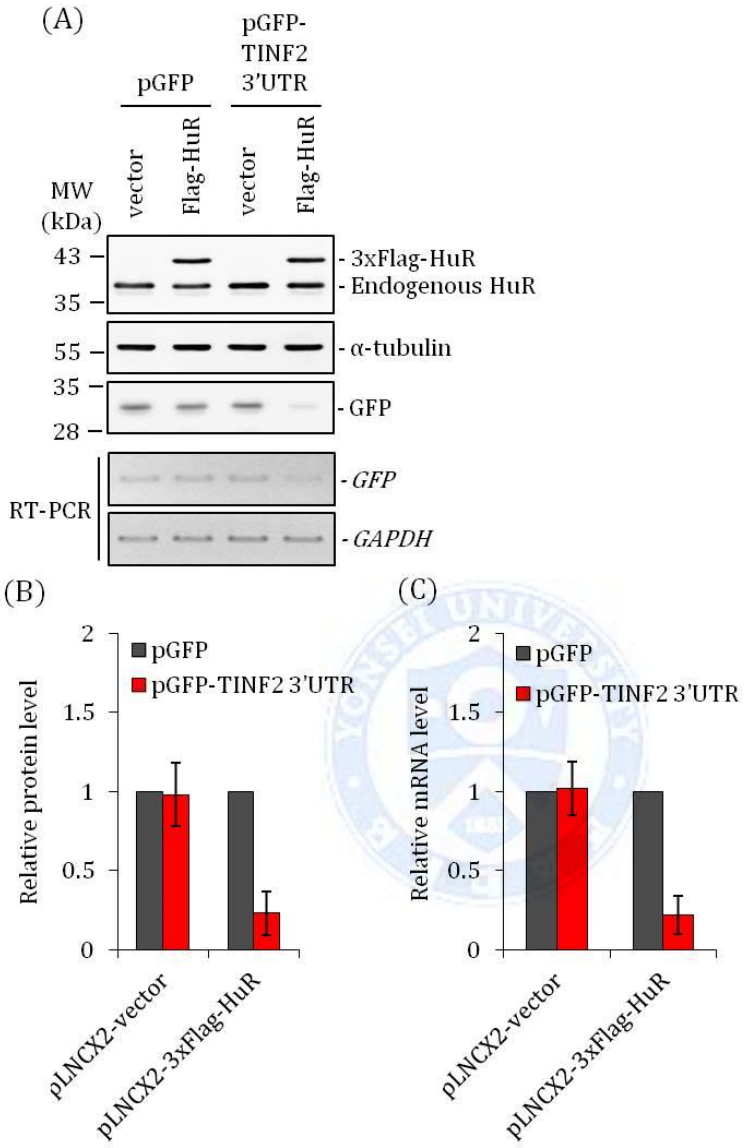
(A)
pGFP
pGFP-TINF2 3'UTR
vector
Flag-HuR
vector
Flag-HuR
MW (kDa)
43
35
55
35
28
- 3xFlag-HuR
- Endogenous HuR
- α-tubulin
- GFP
RT-PCR
- GFP
- GAPDH
(B)
Relative protein level
2
1.5
1
0.5
0
pGFP
pGFP-TINF2 3'UTR
pLNCX2-vector
pLNCX2-3xFlag-HuR
(C)
Relative mRNA level
2
1.5
1
0.5
0
pGFP
pGFP-TINF2 3'UTR
pLNCX2-vector
pLNCX2-3xFlag-HuR

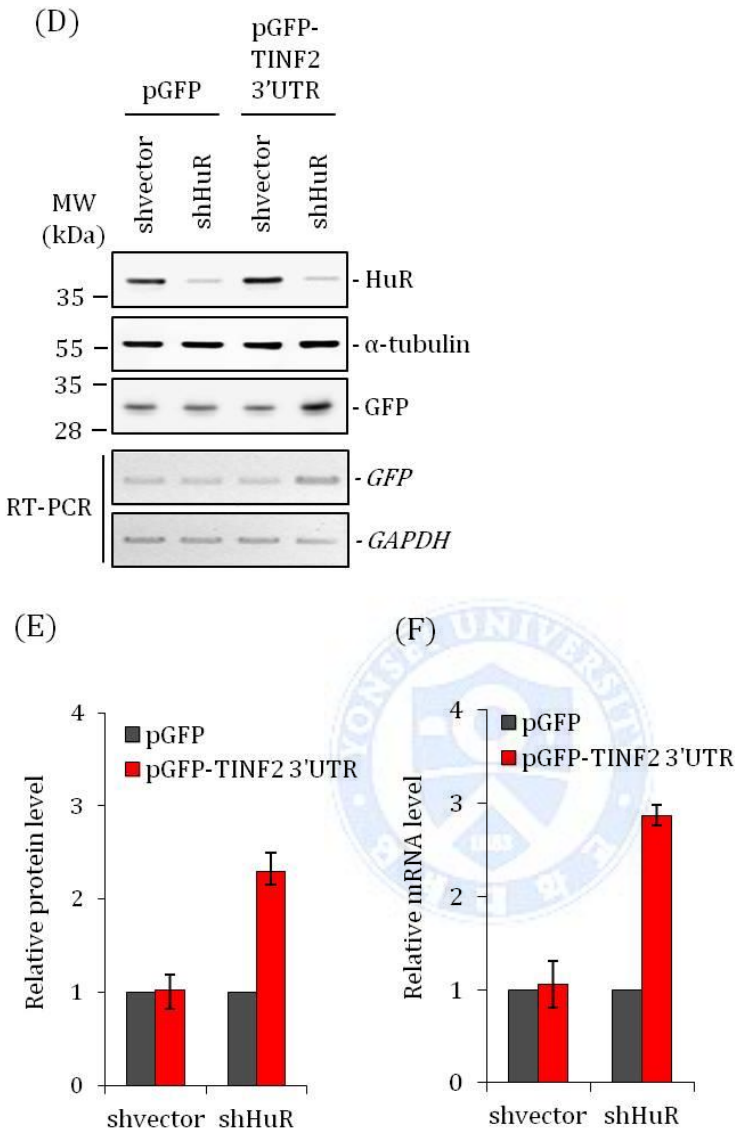

Figure. 5. HuR regulates *TINF2* expression through the *TINF2* 3'UTR.

Figure 5.HuR represses TINF2 expression through 3'UTR of TINF2 mRNA. (A) Plasmid pGFP-TINF2 3′UTR was constructed by attaching the entire TINF2 3′UTR after the GFP coding region. Forty-eight hours after co-transfecting pGFP or pGFP-3′UTR with pLNCX2-vector or pLNCX2-3xFlag-HuR in HeLa CCL2 cells, the levels of reporter GFP protein, HuR, and loading control α-tubulin were measured by the indicated antibodies. Graphical representation of the relative levels of GFP proteins normalized against α-tubulin in (B). The protein levels were quantified with the average and standard deviation from three independent experiments. GFP and chimeric GFP-TINF2 3′UTR mRNAs were measured by RT-PCR. Graphical representation of the relative levels of GFP mRNA normalized against GAPDH in (C). The protein levels were quantified with the average and standard deviation from three independent experiments. (D) Plasmid pGFP-TINF2 3′UTR was constructed by attaching the entire TINF2 3′UTR after the GFP coding region. Forty-eight hours after co-transfecting pGFP or pGFP-3′UTR with shvector or shHuR in HeLa CCL2 cells, the levels of reporter GFP protein, HuR, and loading control α-tubulin were measured by the indicated antibodies. Graphical representation of the relative levels of GFP proteins normalized against α-tubulin in (E). The protein levels were quantified with the average and standard deviation from three independent experiments. GFP and chimeric GFP-TINF2 3′UTR mRNAs were measured by RT-PCR. Graphical representation of the relative levels of GFP mRNA normalized against GAPDH in (F). The protein levels were quantified with the average and standard deviation from three independent experiments.

4.6. Identification of domains in TINF2 3'UTR that are associated with HuR.

As other HuR target mRNAs, TINF2 3´UTR is highly rich in As and Us (Figure 6A). We further investigated the association of HuR with the TINF2 mRNA by testing their association with HuR by RIP-PCR analysis. As binding was restricted to the 3´UTR (Figure 6B), we further subdivided it into four overlapping, ~250-nt fragments and conjugated to GFP chimeric reporters (Figure 6B). Among them, HuR bound to the GFP Full and GFP B regions (Figure 6B and C). Validation of these findings by western blot showed that overexpression of HuR reduced the expression level of GFP in the GFP Full and GFP B from the reporter chimeric plasmid pGFP(3´UTR) (Figure 6D and E). Together, these findings suggested that HuR associated with the TINF2 3´UTR and reduced TINF2 levels by lowering the TINF2 mRNA and by inhibiting its translation.

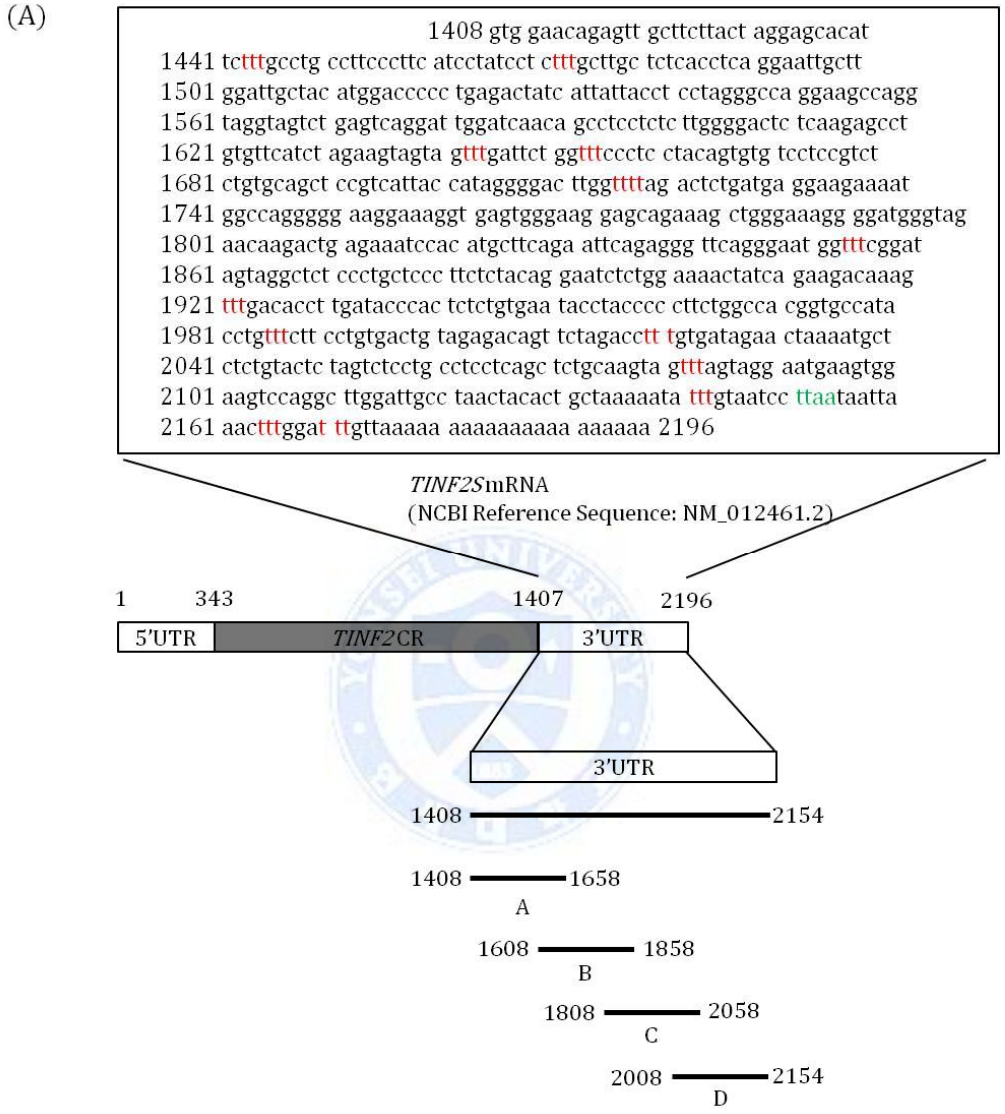

Figure 6. Identification of domains in TINF2 3'UTR that are associated with HuR.

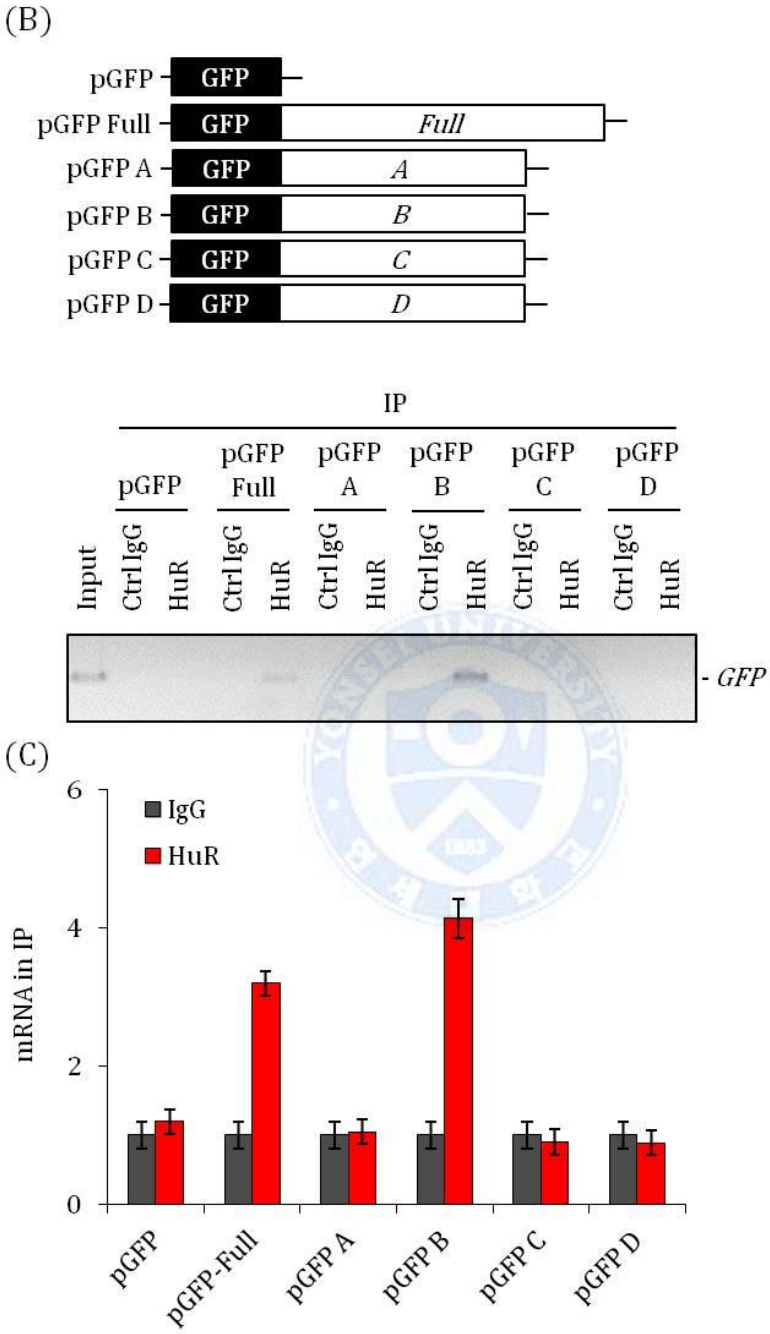

Figure 6. Identification of domains in TINF2 3'UTR that are associated with HuR.

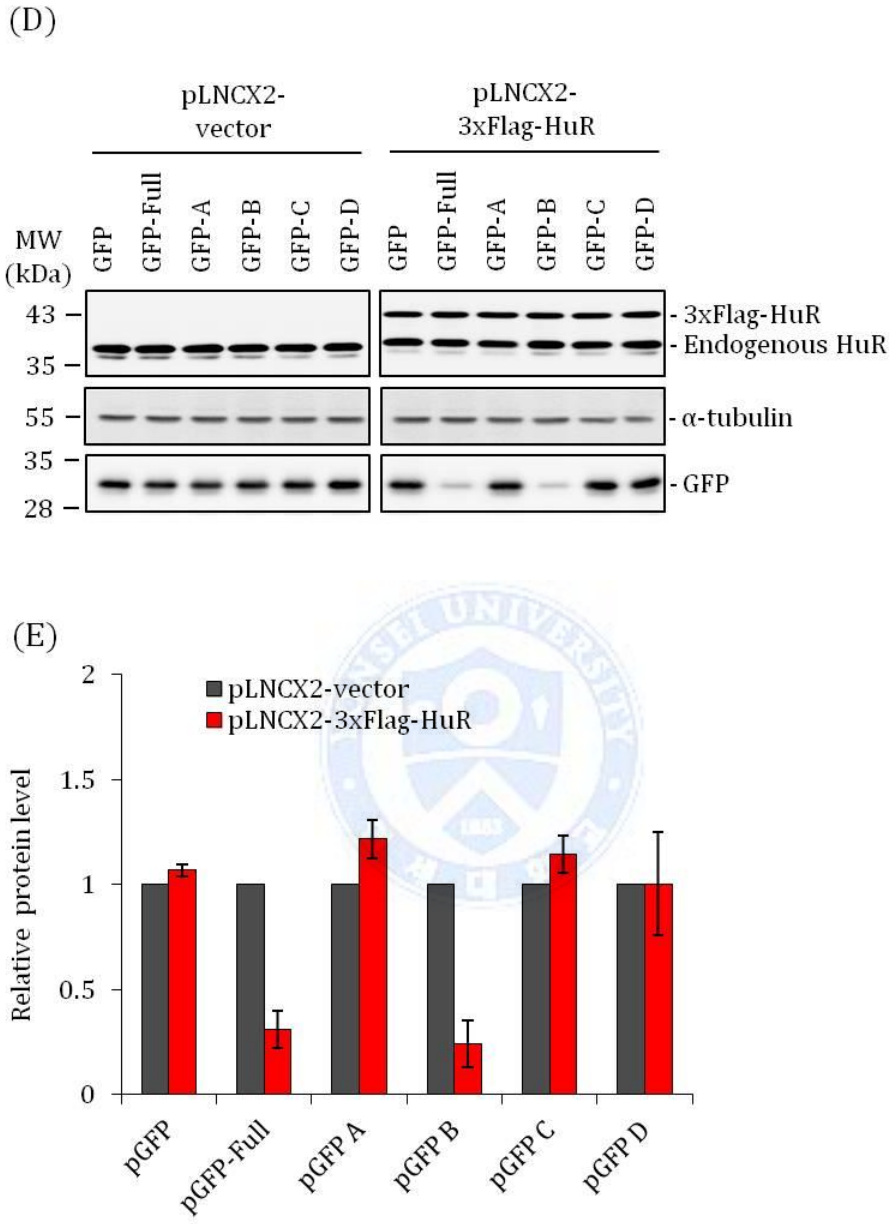

Figure 6. Identification of domains in TINF2 3'UTR that are associated with HuR.

Figure 6. Identification of domains in TINF2 3'UTR that are associated with HuR. (A) Sequence of the AU-rich TINF2 3′UTR. (B) Constructs were prepared to express chimeric RNAs spanning the GFP coding region and each of the four TINF2 3′UTR segments shown in (A). Forty-eight hours after transfection in HeLa CCL2 cells, binding of HuR to each chimeric RNA was tested by RNP-IP, followed by GFP mRNA detection by RT-PCR. Graphical representation of the relative levels of GFP mRNA in HuR IP normalized against IgG IP in (C). The mRNA levels were quantified with the average and standard deviation from three independent experiments. (D) Forty-eight hours after transfection in HeLa CCL2 cells, each chimeric GFP protein levels with overexpressed HuR was tested by Western blot analysis with the indicated antibodies. (E) Graphical representation of the relative levels of GFP protein in overexpressed HuR normalized against a control in (D). The mRNA levels were quantified with the average and standard deviation from three independent experiments.

4.7. Loss of HuR induces cell growth retardation and represses TINF2 mRNA level.

A number of senescence-associated genes include As or Us-rich elements which are known targets to regulate mRNA turnover in their 3' untranslated regions (UTRs), and various transcriptional regulators contribute to coordinate alterations in their mRNA stability (Keene 2007; Simone and Keene 2013; Blackinton and Keene 2014). Alterations in mRNA stability are associated with RNA-binding proteins (RBPs) that enhance or reduce their stabilities. Among RBPs, HuR has been implicated in premature senescence process. Loss of HuR, indicating that HuR expression level and activity are reduced in senescent cells compared to younger cells in primary cells, induces replicative senescence through stabilization of tumor suppressor genes such as p21, p19ARF and p16INK4 in human fibroblasts or murine fibroblasts (Wang et al. 2001; Yi et al. 2010; Pang et al. 2013; Hashimoto et al. 2014). At the same time, deprotection of end chromosomes due to end-replication problem is a hallmark of aging and senescence (Cesare and Karlseder 2012; Cesare et al. 2013). Thus, shelterin, which is composed of six proteins associated with end-protection of chromosomes, also might be a target to be regulated by HuR during senescence, based on that HuR represses mRNA of TINF2 to regulate TINF2 level. To investigate whether HuR regulates expression of shelterin during senescence of primary cells, we first measured HuR levels in early- (PD5) and late-passage (PD23) human caucasian foetal lung fibroblast IMR-90 cells. The standard for passage of IMR-90 cells was based on the logarithmic growth curve and FACS analysis, referring previous observations that five TIFs in intermediate-state telomeres correlate with senescence induction via p53-dependent G1 arrest in human cells (Kaul et al. 2012) (Figure 7A -D). In late-passage cells, HuR levels were reduced in protein level, not in mRNA level (Figure 7E and F). Concomitant with reduction of HuR level, TINF2 levels were enhanced

in mRNA level (Figure 6A and B). During replicative senescence with activated p53 due to uncapped telomere, SIAH1 and TRF2 are upregulated and downregulated, respectively (Fujita et al. 2010). However, we could not observe significant reduction of TRF2 level. Moreover, overexpression of TINF2 stabilizes TRF1 and TRF2 level in protein level (Ye et al. 2004). Under our experimental conditions, we analyzed endogenous shelterin components at intermediate-state telomeres rather than uncapped telomeres, and could not observe significant change level of TRF1 and TRF2.

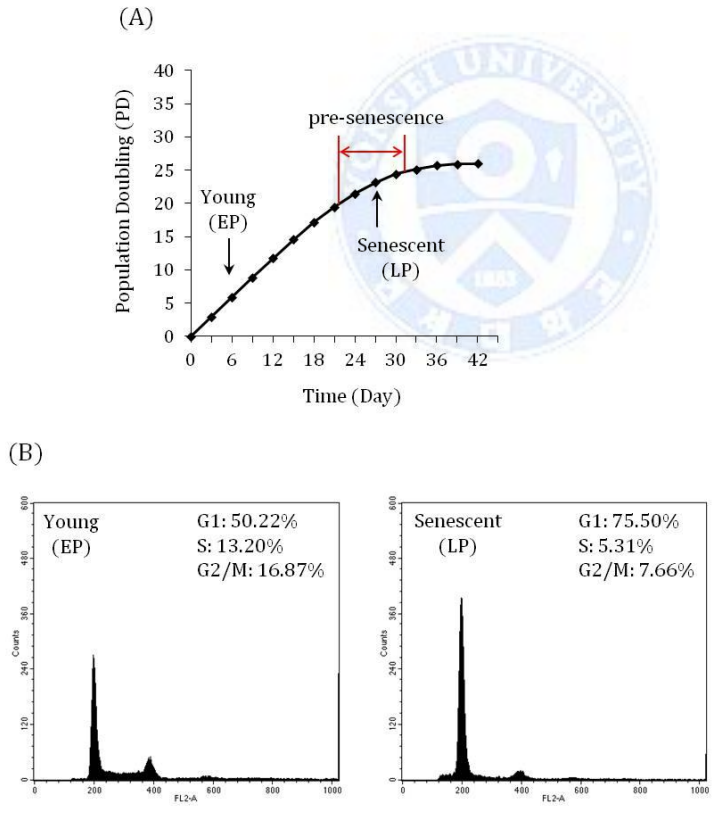

Figure 7. Loss of HuR induces cell growth retardation and represses TINF2 mRNA level.

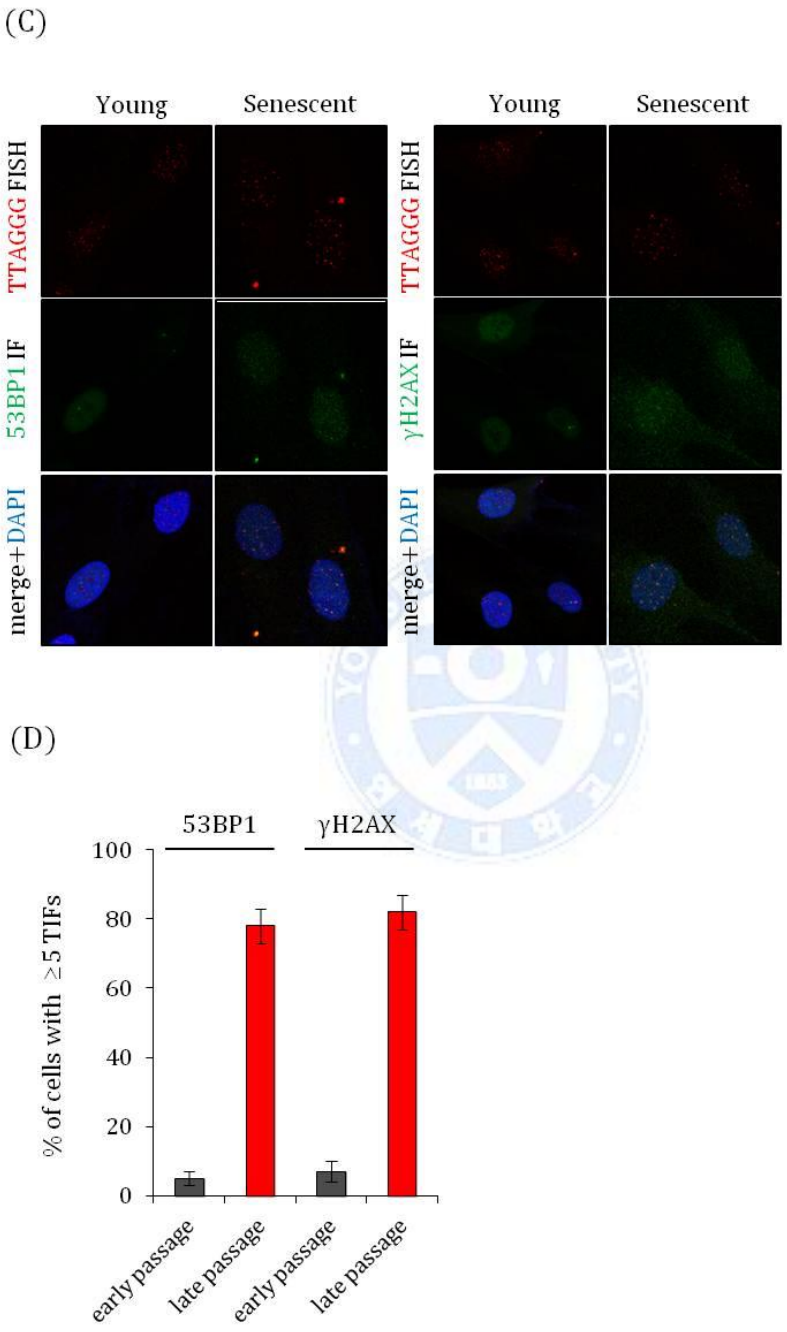

Figure 7. Loss of HuR induces cell growth retardation and represses TINF2 mRNA level.

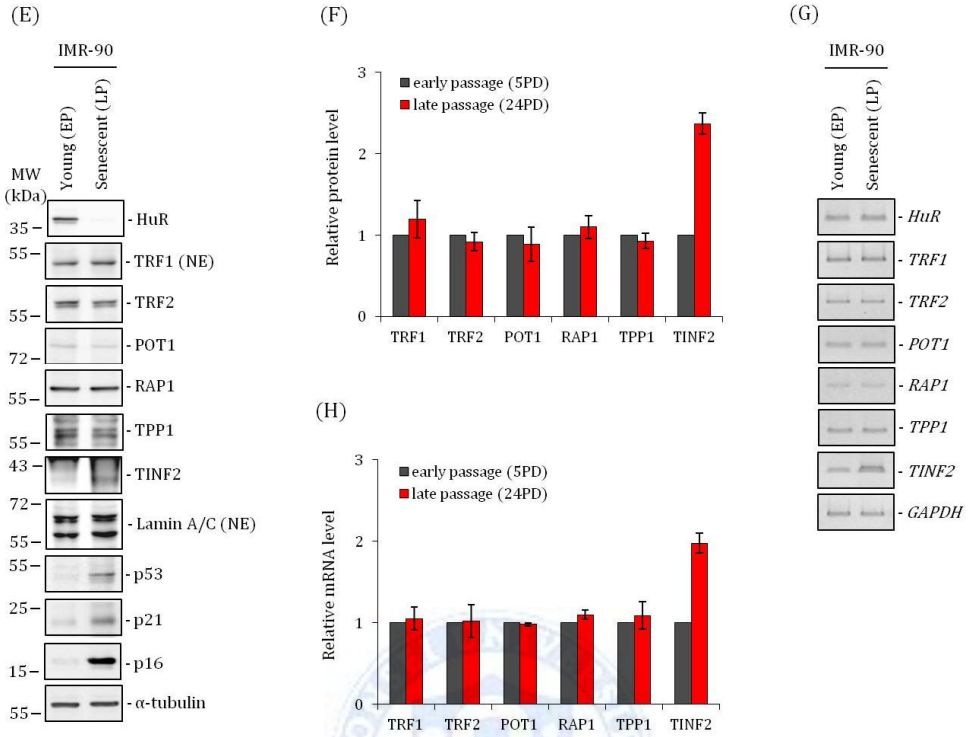

Figure 7. Loss of HuR induces cell growth retardation and represses TINF2 mRNA level.

Figure 7. Loss of HuR induces cell growth retardation and represses TINF2 mRNA level. (A) Growth curve of long-term cultivation of IMR-90 cells. (B) Flow cytometric analysis of IMR-90 cells at early PDs and late PDs. Cells were stained with propidium iodide at early and late PDs, followed by FACS analysis. (C) IMR-90 cells were analysed by PNA-FISH for co-localization of γ -H2AX or 53BP1 foci with telomeric sites marked by TTAGGG-specific FISH probe. Representative fluorescence images of nuclei showing a large number of γ -H2AX or 53BP1 foci are shown as indicated. Immunofluorescence was used to detect γ -H2AX or 53BP1 foci (green), and FISH was used to detect telomeric sites (red). DNA was stained with DAPI in the merged images. A subset of γ -H2AX or 53BP1 foci co-localized with TTAGGG probe is shown. (D) Quantification of TIFs shown in (C). The percentage of cells with >5 γ -H2AX or 53BP1 foci. For each condition, at least 100 cells were counted. (E) IMR-90 cells were collected at different PDs (Early PD, EP; Late PD, LP) and the levels of shelterin componenets (TRF1, TRF2, RAP1, POT1, TPP1 and TINF2), ARFs (p53, p21 and p16) and loading control α-tubulin and Lamin A/C were assessed by Western blot analysis. (F) Graphical representation of the relative levels of shelterin proteins normalized against α-tubulin or Lamin A/C in (E). The protein levels were quantified with the average and standard deviation from three independent experiments. (G) IMR-90 cells were collected at different PDs (Early PD, EP; Late PD, LP) and the levels of shelterin componenets (TRF1, TRF2, RAP1, POT1, TPP1 and TINF2) and PCR loading control GAPDH were assessed by semi-quantitative-RT PCR analysis. (H) Graphical representation of the relative levels of shelterin mRNAs normalized against GAPDH in (G). The protein levels were quantified with the average and standard deviation from three independent experiments.

4.8. HuR depletion upregulates TINF2 expression during cell growth retardation.

Increased levels of TINF2 lead to slight telomere shortening, preventing telomerase from elongating telomeres due to closed-state telomere structure (Kim et al. 2004). To determine whether enhanced TINF2 due to reduction of HuR contributes to the cell growth and the maintenance of telomeres, we stably expressed HuR shRNAs in HeLa S3 cells. During long-term cultivation, HuR levels were stably knockdowned and endogenous TINF2 levels were upregulated (Figure 8E-H). Consistent with previous observations (Wang et al. 2000b; Wang et al. 2001; Mazan-Mamczarz et al. 2003), knockdown of HuR induced premature replicative senescence with p53-dependent G1 arrest through stabilization of ARFs such as p53, p21 and p16 (Figure 8A, B and E-F). Next, to investigate that HuR shRNAs induce dysfunction of telomeres during premature replicative senescence, we performed interphase-TIFs in HeLa S3 HuR shRNA. The results showed that cells containing over five interphase-TIFs were significantly increased without chromosome fusions in shHuR-HeLa S3 cells compared with those in shvector-HeLa S3 cells, indicating that dysfunctional telomeres are induced at intermediate-state telomeres due to the depletion of HuR (Figure 8C and D).

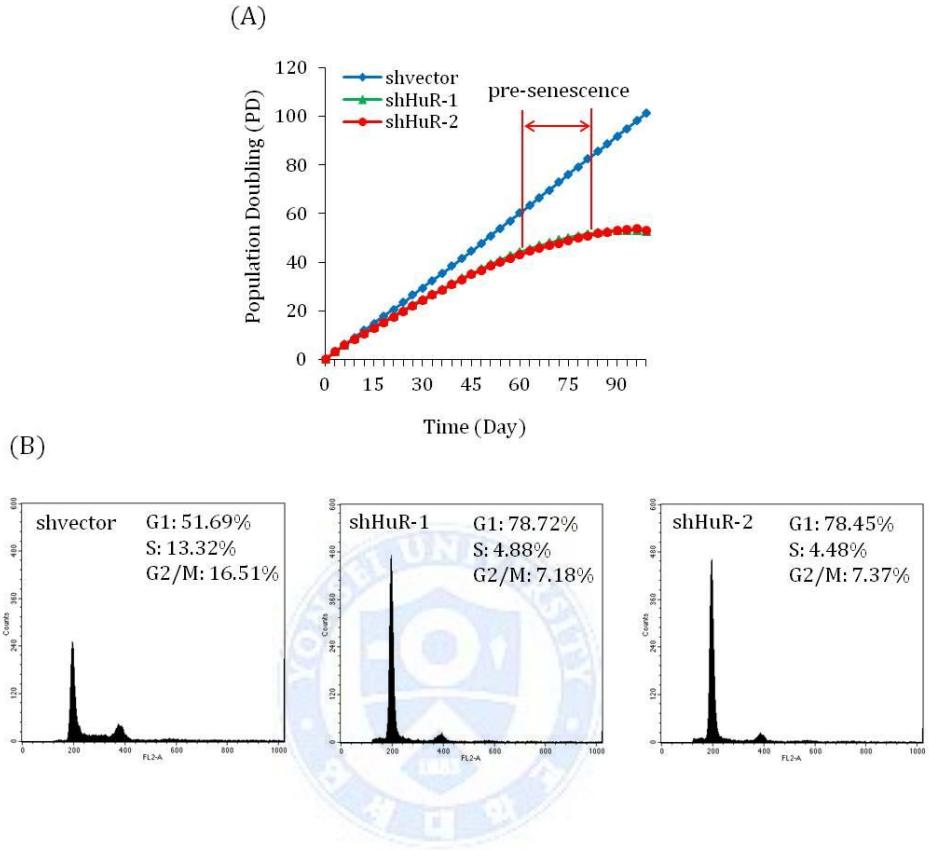

Figure 8. HuR depletion upregulates TINF2 expression during cell growth retardation.

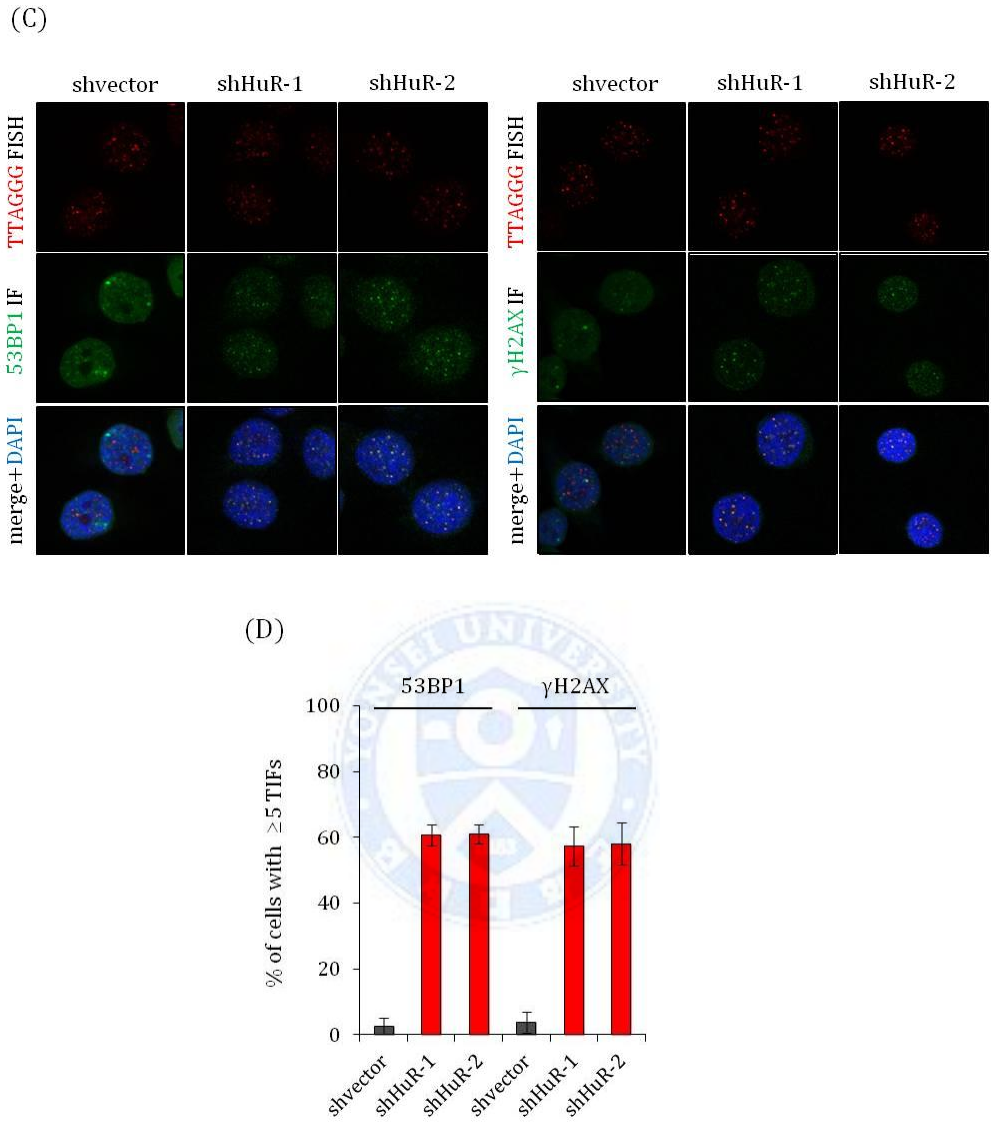

Figure 8. HuR depletion upregulates TINF2 expression during cell growth retardation.

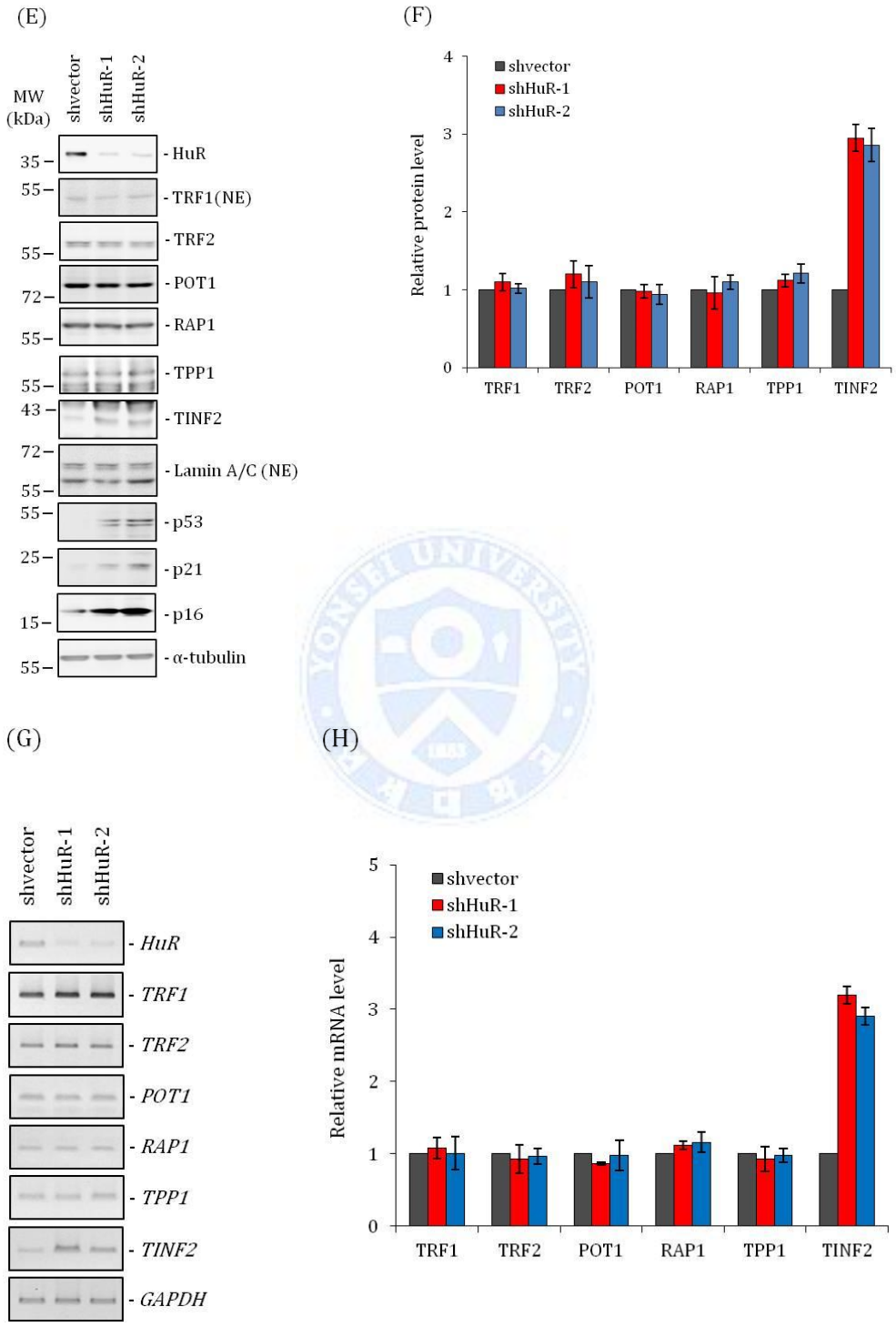

Figure 8. HuR depletion upregulates TINF2 expression during cell growth retardation.

Figure 8. HuR depletion upregulates TINF2 expression during cell growth retardation. (A) Growth curve of long-term cultivation of shvector, shHuR-1 and shHuR-2 HeLa S3 cells. (B) Flow cytometric analysis of HeLa S3 cells at pre-senescent point. Cells were stained with propidium iodide, followed by FACS analysis. (C) HeLa S3 cells were analysed by PNA-FISH for co-localization of γ -H2AX or 53BP1 foci with telomeric sites marked by TTAGGG-specific FISH probe. Representative fluorescence images of nuclei showing a large number of γ -H2AX or 53BP1 foci are shown as indicated. Immunofluorescence was used to detect γ -H2AX or 53BP1 foci (green), and FISH was used to detect telomeric sites (red). DNA was stained with DAPI in the merged images. A subset of γ -H2AX or 53BP1 foci co-localized with TTAGGG probe is shown. (D) Quantification of TIFs shown in (C). The percentage of cells with >5 γ -H2AX or 53BP1 foci. For each condition, at least 100 cells were counted. (E) shvector, shHuR-1 and shHuR-2 HeLa S3 cells were collected at pre-senescent point and the levels of shelterin componenets (TRF1, TRF2, RAP1, POT1, TPP1 and TINF2), ARFs (p53, p21 and p16) and loading control α-tubulin and Lamin A/C were assessed by Western blot analysis. (F) Graphical representation of the relative levels of shelterin proteins normalized against α-tubulin or Lamin A/C in (E). The protein levels were quantified with the average and standard deviation from three independent experiments. (G) shvector, shHuR-1 and shHuR-2 HeLa S3 cells were collected at pre-senescent point and the levels of shelterin componenets (TRF1, TRF2, RAP1, POT1, TPP1 and TINF2) and PCR loading control GAPDH were assessed by semi-quantitative-RT PCR analysis. (H) Graphical representation of the relative levels of shelterin mRNAs normalized against GAPDH in (G). The protein levels were quantified with the average and standard deviation from three independent experiments.

4.9. HuR depletion induces imtermediate-state telomere during senescence.

To address checkpoint activation in IMR-90 cells at pre-senescent point or G1 arrested HeLa S3 cells due to knockdown of HuR, we monitored DNA damage response (ATM-Ser1981 and CHK2-Thr68) and stabilization of ARFs (p53, p21 and p16) at point containing intermediate-state telomeres. The results showed that depletion of HuR activated ATM via phosphorylation at Ser1981, not CHK2 via phosphorylation at Thr68, which is agreement with checkpoint activation to differential DDR from the intermediate-state telomeres, subsequently accumulated p53, p21and p16 (Cesare and Karlseder 2012; Cesare et al. 2013)(Figure 9A and B).

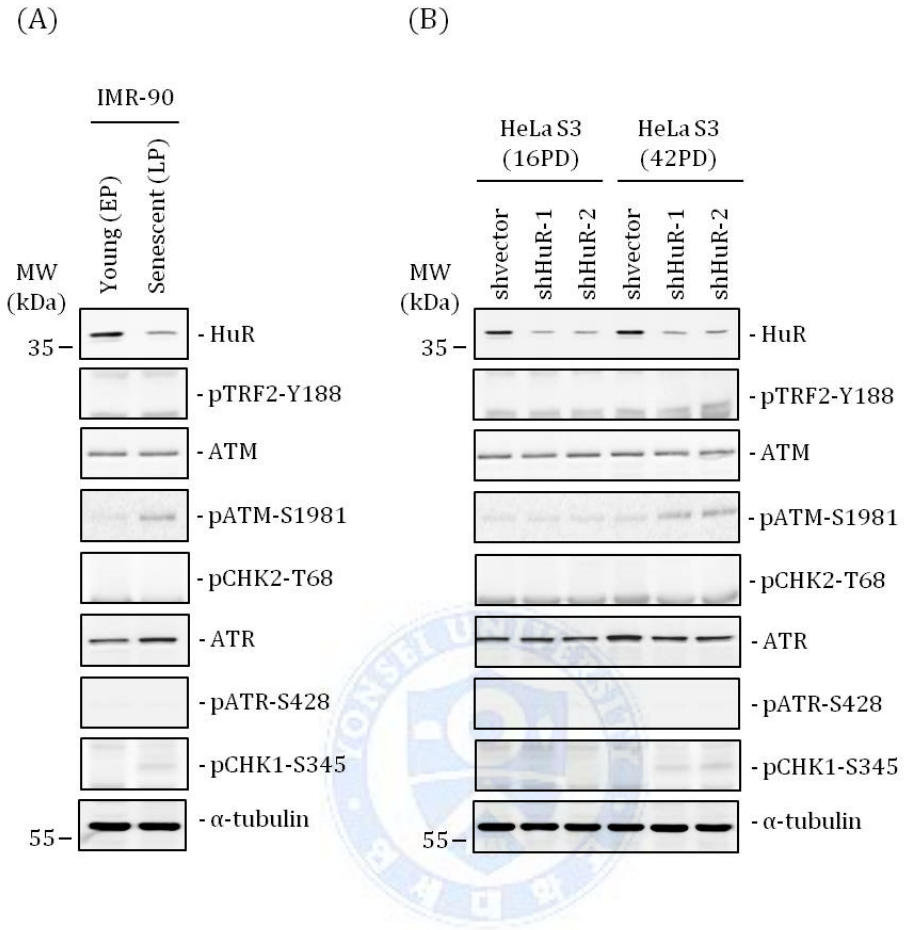

Figure 9. HuR depletion induces imtermediate-state telomere during senescence. (A) and (B) IMR-90 cells and shvector, shHuR-1 and shHuR-2 HeLa S3 cells were collected at early PDs and pre-senescent PDs and the level of checkpoint activation (ATM-Ser1981, ATR-Ser428, CHK2-Thr68 and CHK1-Ser345) and loading control α-tubulin were assessed by Western blot analysis.

5. Discussion

In this study, we discovered that HuR represses TINF2 expression through binding to its 3'UTR in human fibroblasts and cervical adenocarcinoma cell line. Similar to TRF2-mediated telomere-signaling during replicative senescence (Cesare et al. 2013), intermediate-state telomeres were induced by enhanced TINF2 due to reduction of HuR level, suggesting that elevated TINF2 level promotes the higher-order complex with TRF1 and TRF2, and telomere shortening to induce intermediate-state telomeres from closed-state telomeres. Although HuR shRNA activates ATM-Ser1981, knockdown of HuR by shRNA in p53-competent cancer cells or senescent primary cells do not contribute to the G2/M checkpoint (no CHK2-Thr68 phosphorylation). Thus, cells containing intermediate-state telomeres passed through cell division without G2/M checkpoint activation, supporting that telomere-dependent growth arrest is restricted to diploid G1 phase cells.

It is well known that the RBP HuR (human antigen R, a member of the elav/hu family) regulates the stability of numerous target mRNAs and modulates the translation of mRNAs (Hinman and Lou 2008). HuR contains three RNA recognition motifs (RRMs) for binding to 5′ and 3′ untranslated regions (UTRs) of target mRNAs (Keene 2007; Wang et al. 2011; Simone and Keene 2013; Wang et al. 2013). Given the functions of its target mRNAs, HuR has been implicated in processes such as cellular proliferation, cellular senescence, and responses to DNA damage. In particular, reduction of HuR level facilitates senescent process by stabilizing mRNA of the ARF tumor suppressor (Wang et al. 2001; Wang et al. 2003; Yi et al. 2010; Pang et al. 2013; Hashimoto et al. 2014). In this study, we found that knockdown of HuR stabilized TINF2 mRNA to facilitate the higher-order complex, followed by shorten telomeres having characteristics of intermediate-state telomeres which are implicated as the activator of

replicative senescence (Karlseder et al. 2002).

TINF2 is involved in the stabilization of human shelterin and the protection of telomeres (Kim et al. 2004; Liu et al. 2004; Ye and de Lange 2004). Moreover, human TINF2 plays an important role in the regulation of telomere length in telomerase-positive cancer cells (Kim et al. 1999). TINF2 DC mutations, which do not affect the interaction of TINF2 with TRF1, TRF2 and TPP1 among shelterin-binding partners, induce telomere shortening via mechanisms that involve both telomerase-dependent and telomerase-independent pathways (Kocak et al. 2014). However, a role of TINF2 in primary cells has not been fully understood. In this work, during replicative senescence, we observed loss of HuR levels, consistent with previous observations that HuR levels are low in fibroblasts undergoing replicative senescence (Wang et al. 2001; Pang et al. 2013). Loss of HuR reduced senescence-associated gene expression such as cyclin A, cyclin B1 and c-fos (Wang et al. 2001). Moreover, lower level of HuR stabilized ARFs such as p53, p21 and p16 induced replicative senescence (Kawagishi et al. 2013). Here, we found that TINF2 levels were enhanced by reduction of HuR in primary fibroblasts approaching pre-senescene point, and elevated TINF2 facilitated telomere shortening in IMR-90 shHuR (Figure 7 and 8). Thus, HuR plays a critical role in replicative senescence through the stabilization of ARFs, the modulation of senescence-associated gene expression and TINF2-mediated telomere shortening, simultaneously. These results indicate that TINF2 contributes to replicative senescence process.

The uncapped state telomeres are the fusion-sensitive and capable of activating CHK2-Thr68 phosphorylation, as observed in TRF2-deletion murine models (Celli and de Lange 2005). Previous studies have shown that severe knockdown of TRF2 induced canonical DDR signaling in TRF2 shRNA cells and during lifespan extension, indicating canonical DDR from

uncapped-state telomeres and telomere-fusion-dependent genomic instability (Cesare and Karlseder 2012; Cesare et al. 2013). However, mild knockdown of TRF2 induced the differential DDR from intermediate-state telomeres. Differential DDR from telomeres indicates ATM-Ser1981 phosphorylation and no CHK2-Thr68 phosphorylation, which are characteristic properties to mimic DDR from replicative senescence. In this study, knockdown of HuR in cancer cells or reduced HuR in primary fibroblsts activates ATM-Ser1981 phosphorylation, but not CHK2-Thr68 phosphorylation during long-term cultivation. Dysfunctional telomeres due to elevated TINF2 by reduction of HuR coincide with the intermediate-state telomeres from mild knockdown of TRF2. In addition, reduced HuR induced cell growth retardation and arrested cells at G1 phase through the absence of CHK2 activation, consistent with previous observations (Cesare et al. 2013). Overall, these observations demonstrate that deprotection of telomeres due to enhanced TINF2 level by reduction of HuR are closely implicated in the induction of intermediate-state telomere and replicative senescence.

6. References

1. Abreu E, Aritonovska E, Reichenbach P, Cristofari G, Culp B, Terns RM, Lingner J, Terns MP. 2010. TIN2-tethered TPP1 recruits human telomerase to telomeres in vivo. Molecular and cellular biology 30: 2971-2982.

2. Alder JK, Stanley SE, Wagner CL, Hamilton M, Hanumanthu VS, Armanios M. 2015. Exome sequencing identifies mutant TINF2 in a family with pulmonary fibrosis. Chest 147: 1361-1368.

3. Artandi SE. 2006. Telomeres, telomerase, and human disease. The New England journal of medicine 355: 1195-1197.

4. Artandi SE, Attardi LD. 2005. Pathways connecting telomeres and p53 in senescence, apoptosis, and cancer. Biochemical and biophysical research communications 331: 881-890.

5. Bell SP, Dutta A. 2002. DNA replication in eukaryotic cells. Annual review of biochemistry 71: 333-374.

6. Bessler M, Wilson DB, Mason PJ. 2010. Dyskeratosis congenita. FEBS letters 584: 3831-3838.

7. Bhanot M, Smith S. 2012. TIN2 stability is regulated by the E3 ligase Siah2. Molecular and cellular biology 32: 376-384.

8. Blackburn EH. 2001. Switching and signaling at the telomere. Cell 106: 661-673.

9. Blackinton JG, Keene JD. 2014. Post-transcriptional RNA regulons affecting cell cycle and proliferation. Seminars in cell & developmental biology 34: 44-54.

10. Blasco MA. 2005. Telomeres and human disease: ageing, cancer and beyond. Nature reviews Genetics 6: 611-622.

11. Celli GB, de Lange T. 2005. DNA processing is not required for ATM-mediated telomere damage response after TRF2 deletion. Nat Cell Biol 7: 712-718.

12. Cesare AJ, Hayashi MT, Crabbe L, Karlseder J. 2013. The telomere deprotection response is functionally distinct from the genomic DNA damage response. Mol Cell 51: 141-155.

13. Cesare AJ, Karlseder J. 2012. A three-state model of telomere control over human proliferative boundaries. Current opinion in cell biology 24: 731-738.

14. Chen LY, Zhang Y, Zhang Q, Li H, Luo Z, Fang H, Kim SH, Qin L, Yotnda P, Xu J et al. 2012. Mitochondrial localization of telomeric protein TIN2 links telomere regulation to metabolic control. Mol Cell 47: 839-850.

15. Collins K. 2006. The biogenesis and regulation of telomerase holoenzymes. Nature reviews Molecular cell biology 7: 484-494.

16. de Lange T. 2005. Shelterin: the protein complex that shapes and safeguards human telomeres. Genes & development 19: 2100-2110.

17. de Lange T. 2009. How telomeres solve the end-protection problem. Science 326: 948-952.

18. Dean JL, Wait R, Mahtani KR, Sully G, Clark AR, Saklatvala J. 2001. The 3' untranslated region of tumor necrosis factor alpha mRNA is a target of the mRNA-stabilizing factor HuR. Molecular and cellular biology 21: 721-730.

19. Deng Y, Chan S, Chang S. 2008. Telomere dysfunction and tumour suppression: the senescence connection. Nature Reviews Cancer 8: 450-458.

20. Diaz-Munoz MD, Bell SE, Fairfax K, Monzon-Casanova E, Cunningham AF, Gonzalez-Porta M, Andrews SR, Bunik VI, Zarnack K, Curk T et al. 2015. The RNA-binding protein HuR is essential for the B cell antibody response. Nature immunology 16: 415-425.

21. Dormoy-Raclet V, Cammas A, Celona B, Lian XJ, van der Giessen K, Zivojnovic M, Brunelli S, Riuzzi F, Sorci G, Wilhelm BT et al. 2013. HuR and miR-1192 regulate myogenesis by modulating the translation of HMGB1 mRNA. Nature communications 4: 2388.

22. Du HY, Mason PJ, Bessler M, Wilson DB. 2009. TINF2 mutations in children with severe aplastic anemia. Pediatric blood & cancer 52: 687.

23. Durie D, Hatzoglou M, Chakraborty P, Holcik M. 2013. HuR controls mitochondrial morphology through the regulation of Bcl translation. Translation (Austin) 1.

24. Durie D, Lewis SM, Liwak U, Kisilewicz M, Gorospe M, Holcik M. 2011. RNA-binding protein HuR mediates cytoprotection through stimulation of XIAP translation. Oncogene 30: 1460-1469.

25. Dynan WS, Tjian R. 1985. Control of eukaryotic messenger RNA synthesis by sequence-specific DNA-binding proteins. Nature 316: 774-778.

26. Figueroa A, Cuadrado A, Fan J, Atasoy U, Muscat GE, Munoz-Canoves P, Gorospe M, Munoz A. 2003. Role of HuR in skeletal myogenesis through coordinate regulation of muscle differentiation genes. Molecular and cellular biology 23: 4991-5004.

27. Frescas D, de Lange T. 2014a. A TIN2 dyskeratosis congenita mutation causes telomerase-independent telomere shortening in mice. Genes Dev 28: 153-166.

28 Frescas D, de Lange T. 2014b. TRF2-tethered TIN2 can mediate telomere protection by TPP1/POT1. Molecular and cellular biology 34: 1349-1362.

29. Fujita K, Horikawa I, Mondal AM, Jenkins LM, Appella E, Vojtesek B, Bourdon JC, Lane DP, Harris CC. 2010. Positive feedback between p53 and TRF2 during telomere-damage signalling and cellular senescence. Nat Cell Biol 12: 1205-1212.

30. Fukuhara A, Tanino Y, Ishii T, Inokoshi Y, Saito K, Fukuhara N, Sato S, Saito J, Ishida T, Yamaguchi H et al. 2013. Pulmonary fibrosis in dyskeratosis congenita with TINF2 gene mutation. The European respiratory journal 42: 1757-1759.

31. Gerstberger S, Hafner M, Tuschl T. 2014. A census of human RNA-binding proteins. Nat Rev Genet 15: 829-845.

32. Ghosh M, Aguila HL, Michaud J, Ai Y, Wu MT, Hemmes A, Ristimaki A, Guo C, Furneaux H, Hla T. 2009. Essential role of the RNA-binding protein HuR in progenitor cell survival in mice. The Journal of clinical investigation 119: 3530-3543.

33. Gleeson M, O'Marcaigh A, Cotter M, Brosnahan D, Vulliamy T, Smith OP. 2012. Retinal vasculopathy in autosomal dominant dyskeratosis congenita due to TINF2 mutation. Br J Haematol 159: 498.

34. Gorospe M. 2003. HuR in the mammalian genotoxic response: post-transcriptional multitasking. Cell cycle 2: 412-414.

35. Hashimoto M, Tsugawa T, Kawagishi H, Asai A, Sugimoto M. 2014. Loss of HuR leads to senescence-like cytokine induction in rodent fibroblasts by activating NF-kappaB. Biochimica et biophysica acta 1840: 3079-3087.

36. Hinman MN, Lou H. 2008. Diverse molecular functions of Hu proteins. Cellular and molecular life sciences : CMLS 65: 3168-3181.

37. Kabir S, Hockemeyer D, de Lange T. 2014. TALEN gene knockouts reveal no requirement for the conserved human shelterin protein Rap1 in telomere protection and length regulation. Cell reports 9: 1273-1280.

38. Kaminker P, Plachot C, Kim SH, Chung P, Crippen D, Petersen OW, Bissell MJ, Campisi J, Lelievre SA. 2005. Higher-order nuclear organization in growth arrest of human mammary

epithelial cells: a novel role for telomere-associated protein TIN2. Journal of cell science 118: 1321-1330.

39. Karlseder J, Smogorzewska A, de Lange T. 2002. Senescence induced by altered telomere state, not telomere loss. Science 295: 2446-2449.

40. Katsanou V, Milatos S, Yiakouvaki A, Sgantzis N, Kotsoni A, Alexiou M, Harokopos V, Aidinis V, Hemberger M, Kontoyiannis DL. 2009. The RNA-binding protein Elavl1/HuR is essential for placental branching morphogenesis and embryonic development. Molecular and cellular biology 29: 2762-2776.

41. Kaul Z, Cesare AJ, Huschtscha LI, Neumann AA, Reddel RR. 2012. Five dysfunctional telomeres predict onset of senescence in human cells. EMBO reports 13: 52-59.

42. Kawagishi H, Hashimoto M, Nakamura H, Tsugawa T, Watanabe A, Kontoyiannis DL, Sugimoto M. 2013. HuR maintains a replicative life span by repressing the ARF tumor suppressor. Molecular and cellular biology 33: 1886-1900.

43. Keene JD. 2007. RNA regulons: coordination of post-transcriptional events. Nat Rev Genet 8: 533-543.

44. Keene JD, Komisarow JM, Friedersdorf MB. 2006. RIP-Chip: the isolation and identification of mRNAs, microRNAs and protein components of ribonucleoprotein complexes from cell extracts. Nature protocols 1: 302-307.

45. Kim HH, Abdelmohsen K, Gorospe M. 2010. Regulation of HuR by DNA Damage Response Kinases. Journal of nucleic acids 2010.

46. Kim HH, Gorospe M. 2008. Phosphorylated HuR shuttles in cycles. Cell cycle 7: 3124-3126.

47. Kim HH, Kuwano Y, Srikantan S, Lee EK, Martindale JL, Gorospe M. 2009. HuR recruits let-7/RISC to repress c-Myc expression. Genes Dev 23: 1743-1748.

48. Kim I, Hur J, Jeong S. 2015. HuR represses Wnt/beta-catenin-mediated transcriptional activity by promoting cytoplasmic localization of beta-catenin. Biochem Biophys Res Commun 457: 65-70.

49. Kim SH, Beausejour C, Davalos AR, Kaminker P, Heo SJ, Campisi J. 2004. TIN2 mediates functions of TRF2 at human telomeres. The Journal of biological chemistry 279: 43799-43804.

50. Kim SH, Davalos AR, Heo SJ, Rodier F, Zou Y, Beausejour C, Kaminker P, Yannone SM, Campisi J. 2008. Telomere dysfunction and cell survival: roles for distinct TIN2-containing complexes. J Cell Biol 181: 447-460.

51. Kim SH, Kaminker P, Campisi J. 1999. TIN2, a new regulator of telomere length in human cells. Nat Genet 23: 405-412.

52. Kocak H, Ballew BJ, Bisht K, Eggebeen R, Hicks BD, Suman S, O'Neil A, Giri N, Maillard I, Alter BP et al. 2014. Hoyeraal-Hreidarsson syndrome caused by a germline mutation in the TEL patch of the telomere protein TPP1. Genes Dev 28: 2090-2102.

53. Lal S, Burkhart RA, Beeharry N, Bhattacharjee V, Londin ER, Cozzitorto JA, Romeo C, Jimbo M, Norris ZA, Yeo CJ et al. 2014. HuR posttranscriptionally regulates WEE1: implications for the DNA damage response in pancreatic cancer cells. Cancer research 74: 1128-1140.

54. Leandersson K, Riesbeck K, Andersson T. 2006. Wnt-5a mRNA translation is suppressed by the Elav-like protein HuR in human breast epithelial cells. Nucleic acids research 34: 3988-3999.

55. Lebedeva S, Jens M, Theil K, Schwanhausser B, Selbach M, Landthaler M, Rajewsky N. 2011. Transcriptome-wide analysis of regulatory interactions of the RNA-binding protein HuR. Mol Cell 43: 340-352.

56. Liu D, O'Connor MS, Qin J, Songyang Z. 2004. Telosome, a mammalian telomere-associated complex formed by multiple telomeric proteins. The Journal of biological chemistry 279: 51338-51342.

57. Liu L, Christodoulou-Vafeiadou E, Rao JN, Zou T, Xiao L, Chung HK, Yang H, Gorospe M, Kontoyiannis D, Wang JY. 2014. RNA-binding protein HuR promotes growth of small intestinal mucosa by activating the Wnt signaling pathway. Molecular biology of the cell 25: 3308-3318.

58. Lopez de Silanes I, Fan J, Yang X, Zonderman AB, Potapova O, Pizer ES, Gorospe M. 2003. Role of the RNA-binding protein HuR in colon carcinogenesis. Oncogene 22: 7146-7154.

59. Lopez de Silanes I, Stagno d'Alcontres M, Blasco MA. 2010. TERRA transcripts are bound by a complex array of RNA-binding proteins. Nature communications 1: 33.

60. Lunde BM, Moore C, Varani G. 2007. RNA-binding proteins: modular design for efficient function. Nat Rev Mol Cell Biol 8: 479-490.

61. Marcand S, Brevet V, Mann C, Gilson E. 2000. Cell cycle restriction of telomere elongation. Current biology 10: 487-490.

62. Martinez P, Blasco MA. 2011. Telomeric and extra-telomeric roles for telomerase and the telomere-binding proteins. Nat Rev Cancer 11: 161-176.

63. Mazan-Mamczarz K, Galban S, Lopez de Silanes I, Martindale JL, Atasoy U, Keene JD, Gorospe M. 2003. RNA-binding protein HuR enhances p53 translation in response to ultraviolet light irradiation. Proc Natl Acad Sci U S A 100: 8354-8359.

64. Mitchell JR, Wood E, Collins K. 1999. A telomerase component is defective in the human disease dyskeratosis congenita. Nature 402: 551-555.

65. Moore MJ. 2005. From birth to death: the complex lives of eukaryotic mRNAs. Science 309: 1514-1518.

66. O'Connor MS, Safari A, Xin H, Liu D, Songyang Z. 2006. A critical role for TPP1 and TIN2 interaction in high-order telomeric complex assembly. Proc Natl Acad Sci U S A 103: 11874-11879.

67. Pang L, Tian H, Chang N, Yi J, Xue L, Jiang B, Gorospe M, Zhang X, Wang W. 2013. Loss of CARM1 is linked to reduced HuR function in replicative senescence. BMC molecular biology 14: 15.

68. Paukku K, Backlund M, De Boer RA, Kalkkinen N, Kontula KK, Lehtonen JY. 2012. Regulation of AT1R expression through HuR by insulin. Nucleic acids research 40: 5250-5261.

Peng SS, Chen CY, Xu N, Shyu AB. 1998. RNA stabilization by the AU-rich element binding protein, HuR, an ELAV protein. The EMBO journal 17: 3461-3470.

69. Sarper N, Zengin E, Kilic SC. 2010. A child with severe form of dyskeratosis congenita and TINF2 mutation of shelterin complex. Pediatric blood & cancer 55: 1185-1186.

70. Sasa GS, Ribes-Zamora A, Nelson ND, Bertuch AA. 2012. Three novel truncating TINF2 mutations causing severe dyskeratosis congenita in early childhood. Clinical genetics 81: 470-478.

71. Saunus JM, French JD, Edwards SL, Beveridge DJ, Hatchell EC, Wagner SA, Stein SR, Davidson A, Simpson KJ, Francis GD et al. 2008. Posttranscriptional regulation of the breast cancer susceptibility gene BRCA1 by the RNA binding protein HuR. Cancer research 68: 9469-9478.

72. Savage SA, Giri N, Baerlocher GM, Orr N, Lansdorp PM, Alter BP. 2008a. TINF2, a component of the shelterin telomere protection complex, is mutated in dyskeratosis congenita. Am J Hum Genet 82: 501-509.

73. Savage SA. 2008b. TINF2, a component of the shelterin telomere protection complex, is mutated in dyskeratosis congenita. American journal of human genetics 82: 501-509.

74. Simone LE, Keene JD. 2013. Mechanisms coordinating ELAV/Hu mRNA regulons. Current opinion in genetics & development 23: 35-43.

75. Singh M, Martinez AR, Govindaraju S, Lee BS. 2013. HuR inhibits apoptosis by amplifying Akt signaling through a positive feedback loop. Journal of cellular physiology 228: 182-189.

76. Srikantan S, Tominaga K, Gorospe M. 2012. Functional interplay between RNA-binding protein HuR and microRNAs. Current protein & peptide science 13: 372-379.

77. Sullivan LB, Santos JH, Chandel NS. 2012. Mitochondria and telomeres: the promiscuous roles of TIN2. Mol Cell 47: 823-824.

78. Takai KK, Kibe T, Donigian JR, Frescas D, de Lange T. 2011. Telomere protection by TPP1/POT1 requires tethering to TIN2. Mol Cell 44: 647-659.

79. Topisirovic I, Siddiqui N, Orolicki S, Skrabanek LA, Tremblay M, Hoang T, Borden KL. 2009. Stability of eukaryotic translation initiation factor 4E mRNA is regulated by HuR, and this activity is dysregulated in cancer. Molecular and cellular biology 29: 1152-1162.

80. Tsangaris E, Adams SL, Yoon G, Chitayat D, Lansdorp P, Dokal I, Dror Y. 2008. Ataxia and pancytopenia caused by a mutation in TINF2. Human genetics 124: 507-513.

81. Walne AJ, Dokal I. 2009. Advances in the understanding of dyskeratosis congenita. British journal of haematology 145: 164-172.

82. Walne AJ, Vulliamy T, Beswick R, Kirwan M, Dokal I. 2008. TINF2 mutations result in very short telomeres: analysis of a large cohort of patients with dyskeratosis congenita and related bone marrow failure syndromes. Blood 112: 3594-3600.

83. Wang H, Li H, Shi H, Liu Y, Liu H, Zhao H, Niu L, Teng M, Li X. 2011. Preliminary crystallographic analysis of the RNA-binding domain of HuR and its poly(U)-binding properties. Acta crystallographica Section F, Structural biology and crystallization communications 67: 546-550.

84. Wang H, Zeng F, Liu Q, Liu H, Liu Z, Niu L, Teng M, Li X. 2013. The structure of the ARE-binding domains of Hu antigen R (HuR) undergoes conformational changes during RNA binding. Acta crystallographica Section D, Biological crystallography 69: 373-380.

85. Wang W, Caldwell MC, Lin S, Furneaux H, Gorospe M. 2000a. HuR regulates cyclin A and cyclin B1 mRNA stability during cell proliferation. The EMBO journal 19: 2340-2350.

86. Wang W, Furneaux H, Cheng H, Caldwell MC, Hutter D, Liu Y, Holbrook N, Gorospe M. 2000b. HuR regulates p21 mRNA stabilization by UV light. Molecular and cellular biology 20: 760-769.

87. Wang W, Yang X, Cristofalo VJ, Holbrook NJ, Gorospe M. 2001. Loss of HuR is linked to reduced expression of proliferative genes during replicative senescence. Molecular and cellular biology 21: 5889-5898.

88. Wang W, Yang X, Lopez de Silanes I, Carling D, Gorospe M. 2003. Increased AMP:ATP ratio and AMP-activated protein kinase activity during cellular senescence linked to reduced HuR function. The Journal of biological chemistry 278: 27016-27023.

89. Weinrich SL, Pruzan R, Ma L, Ouellette M, Tesmer VM, Holt SE, Bodnar AG, Lichtsteiner S, Kim NW, Trager JB et al. 1997. Reconstitution of human telomerase with the template RNA component hTR and the catalytic protein subunit hTRT. Nature Genetics 17: 498-502.

90. Yamada K, Yagihashi A, Yamada M, Asanuma K, Moriai R, Kobayashi D, Tsuji N, Watanabe N. 2002. Decreased gene expression for telomeric-repeat binding factors and TIN2 in malignant hematopoietic cells. Anticancer research 22: 1315-1320.

91. Yamaguchi H, Inokuchi K, Takeuchi J, Tamai H, Mitamura Y, Kosaka F, Ly H, Dan K. 2010. Identification of TINF2 gene mutations in adult Japanese patients with acquired bone marrow failure syndromes. Br J Haematol 150: 725-727.

92. Yang D, He Q, Kim H, Ma W, Songyang Z. 2011. TIN2 protein dyskeratosis congenita missense mutants are defective in association with telomerase. The Journal of biological chemistry 286: 23022-23030.

93. Ye JZ, de Lange T. 2004. TIN2 is a tankyrase 1 PARP modulator in the TRF1 telomere length control complex. Nat Genet 36: 618-623.

94. Ye JZ, Donigian JR, van Overbeek M, Loayza D, Luo Y, Krutchinsky AN, Chait BT, de Lange T. 2004. TIN2 binds TRF1 and TRF2 simultaneously and stabilizes the TRF2 complex on telomeres. The Journal of biological chemistry 279: 47264-47271.

95. Yi J, Chang N, Liu X, Guo G, Xue L, Tong T, Gorospe M, Wang W. 2010. Reduced nuclear export of HuR mRNA by HuR is linked to the loss of HuR in replicative senescence. Nucleic acids research 38: 1547-1558.

7. Summary (Korean)

텔로머레이즈에 의한 세포 주기조절에서 NOL1 기능 분석 및 HuR에 의한 텔로미어 결합단백질 TINF2 mRNA 분해 기작 연구

연세대학교 대학원

융합오믹스 의생명과학과

홍주영

인간의 텔로머레이즈는 염색체 말단의 telomeric DNA repeats (TTAGGG)을 합성하는 ribonucleoprotein (RNP) complex이다. 정상 체세포에서의 텔로머레이즈의 역할은 노화를 극복하고 수명을 연장하는 것으로 충분하지만, 종양 세포에서의 텔로머레이즈는 텔로미어를 연장하는 것 말고도 그 외의 다른 활성을 갖는 것으로 알려져있다. 이 연구에서 우리는 NOL1(proliferation-associated nuclear antigen p120)이 TERC를 통해 catalically active 텔로머레이즈와 결합하는 것을 보여준다. 또한, 우리는 NOL1은 cyclin D1의 프로모터에 결합하여 전사를 활성화시키는 것뿐 만 아니라, 텔로머레이즈 역시 NOL1과 결합함으로써 cyclin D1의 프로모터에 결합하고 전사를 활성화시키는 것을 보여준다. 이는 텔로머레이즈가 NOL1 의존적으로 cyclin D1의 전사를 조절한다는 것을 말해준다. 이 연구에서

우리는 NOL1에 의해 텔로머레이즈가 암세포의 생존과 성장 유지에 있어서 중요한 성장 촉진 유전자들의 발현을 강화시킨 다는 것을 보여준다. 따라서, NOL1과 텔로머레이즈의 상호작용을 통해 계속적으로 세포가 분열할 수 있게 함으로써, 텔로머레이즈의 non-canonical 기능이 암화 과정에 중요하다는 것을 밝혀냈다.

짧은 텔로미어 길이와 ARF 암 억제 유전자들의 안정화는 노화과정에서 보이는 특징적인 속성이다. Primary 세포에서 텔로미어는 불완전 DNA 복제 기작으로 인해 점점 짧아지는 동시에, ARF 암 억제 유전자들은 mRNA turnover나 번역과 같은 전사 후 조절과정을 통해 조절된다. 그러한 조절 과정은 목표 유전자의 발현을 선택적으로 조절하는 RNA 결합 단백질이 작용하게 된다. 그 중, elav/hu family인 HuR가 ARF 암 억제 유전자들의 mRNA를 안정화시킴으로써 노화 과정을 촉진시킨다. 그러나, HuR에 의한 ARF 암 억제 유전자들의 안정화와 노화과정에서의 텔로미어 길이 단축에 대한 정확한 연관성은 아직 잘 연구되지 않았다. 여기서, 우리는 HuR가 TINF2(TRF1-Interacting Nuclear Factor 2)의 3'UTR에 결합함으로써 발현을 억제시킨다는 것을 발견하였다. HuR의 발현감소는 TINF2의 mRNA를 안정화시켜, 곧 텔로미어 단축을 가속화시킨다. 또한, 가속화된 텔로미어 단축효과는 ARF 암 억제 유전자들의 안정화로 인한 세포 주기 차단 에 앞서 그 이전에 발생한다는 것을 밝혀냈다. 따라서, 우리의 연구는 HuR에 조절에 따라 ARF 암 억제 유전자의 안정화와 점진적인 텔로미어의 길이 단축과정이 노화과정에 동시에 수반된다는 것을 밝혀냈다.

핵심이 되는 말; Telomerase, NOL1, Cell cycle, Cyclin D1, Telomere, TINF2, HuR